Dynamic model of a ball bearing, vibration analysis

Final Project

Université de Picardie Jules Verne, Amiens, France

Martín Torrego, Marcos

Tutor: Henao, Humberto

July 2015

Abstract

This paper presents a simulation model for a ball bearing test rig, where different ways of operating can be implemented. This has been done using a time-varying, non-linear bearing model obtained in the bibliography. The present model is explained carefully so the misunderstood questions in the present bibliography can be solve and facilitate future works.

The model presented is part of a bigger project which objective is simulating faults in ball bearings and gears to support an electric motor. Additionally, the results of this analyse would be available to see their effects over this motor, as the most important part of the electromechanical complex system.

The numerical and graphic results showed here give an explanation of the performance of the dynamic and kinematic of a 2 d.o.f. ball bearing model for three and nine balls.

Acknowledgments

This research has been supported by the Laboratory for Innovative Technologies (Laboratoire des Technologies Innovantes - LTI), EESA team, within the fold of the Université de Picardie Jules Verne. I am very grateful to both, this university and my home-university, University of Valladolid, to be able to manage this Erasmus scholarship.

I would like to show my gratitude for the support and the widespread knowledge of the tutor of the project, Mr Humberto Henao, who have deeply contributed to the development of the models and research work. Not only him, but also the colleges of the laboratory have been close to me during this project so I fell very thankful for their assistance and friendship.

During these studies abroad I have known new people in my life who has become part of my family during this period. So I am immensely grateful for those funny and great moments that we have being together.

Finally, special thanks to my family. Words cannot express how grateful I am to my parents and siblings whose support in the distance, and not only in the distance, have made me stronger and decided to strive towards my goal.

Table of contents

Index of Figures

1. INTRODUCTION

Frame of the project

In the field of the engineering, when a device or machine is designed, it is conceived to be as durable and robust as possible. However, that life is limited and in medium complexity machines their behaviour during their lives is unclear. Maintenance of machines is a well-known activity in the industry and, since the Second Industrial Revolution in the beginning of the 19th century, it has undergone thanks to different methods.

Maintenance has a big relevance for ball bearings due to the different problems associated to their spoilage. Ball bearings are used to hold big rotate loads and the problems that we can detect are noise, vibrations, which can finish in a fault of stability, a reduction of the efficiency of the whole system or the deterioration of the machine held or the typically used gearbox. Definitely, the worst problem that can occur is a breakdown of the machine that, in ball bearings usually mean also a breakdown or a big damage of the main machine.

As Marín [1] consider, detect a trouble in a machine before it happens and causes a breakdown in a higher system have always been a worry for the maintenance managers. So, historically, different strategies of maintenance have been followed. Depending on the sort of execution, the maintenance can be classified by:

- Corrective maintenance, which develops activities to detect, isolates and rectify a fault so that the failed machine can be restored to its normal operable state. This sometimes means doing an emergency stop. In Figure 1.1 we can see how the costs are increased punctually when a fault occurs as it is shown in Keith Mobley [2]

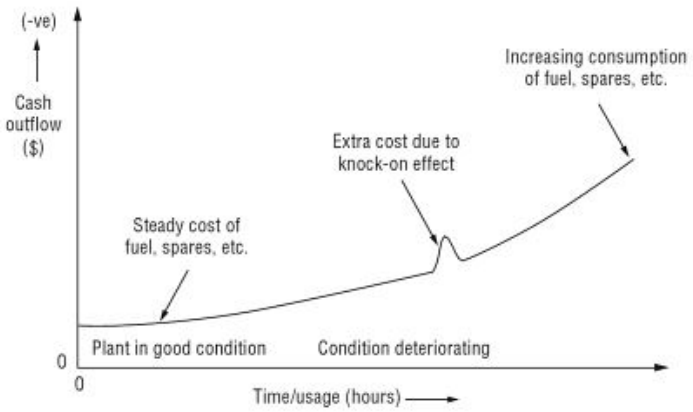

Figure 1. 1 Typical cost of a deterioration in plant condition

- Preventive maintenance, where the substitution of pieces that can cause failures are changed with certain periodicity. These periods are based on statistical criteria. The possibility to choose when this maintenance will be made is the biggest advantage of the preventive maintenance. The disadvantage is the replacement of pieces that can still work for some time or the fail of pieces that have not reach the useful life expected. Figure 2 shows the temporary evolution of an example plant which mainly uses this preventive maintenance.

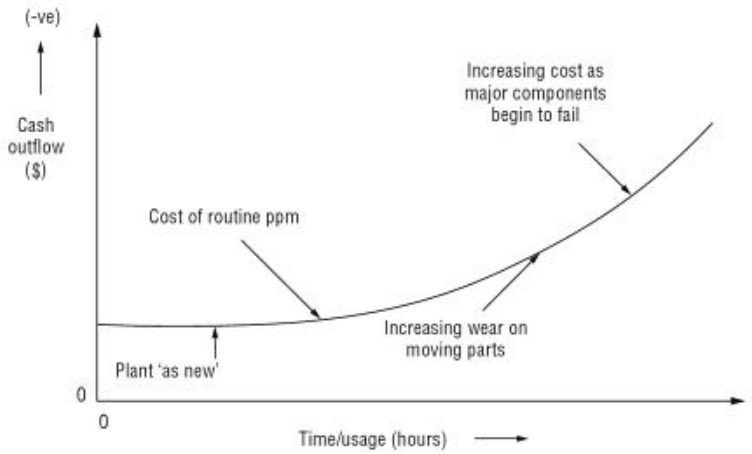

Figure 1. 2 Typical cost of a preventive maintenance strategy

- Predictive maintenance could be defined as the organized surveillance with periodic or continuous measures of system state variables and its comparison with established patterns, to determine the instant when a maintenance intervention must be done.

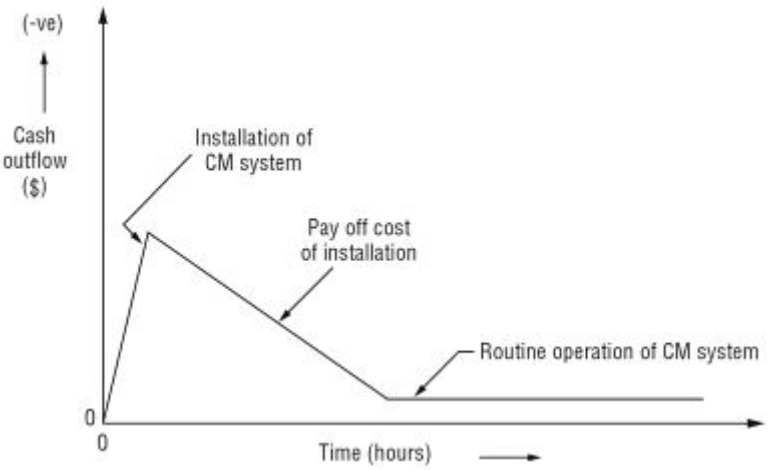

Figure 1. 3 Typical overall cash flow from an investment in predictive maintenance.

There are several applying technics of surveillance and diagnostic for the predictive maintenance: thermic analysis, study of lubricant composition, vibration analysis, ultrasonic examination... After all, the most used technic to do rotating machines diagnostics is vibration analysis, due to the possibility of obtaining information of the energy flow through the supporting elements and elemental torques of the machine, which can show the fault level.

According to Ballesteros [3], when a predictive strategy of maintenance is applied, the useful life of an asset is up to five times longer than applying a preventive strategy. The corrective (reactive) strategy is the maintenance strategy that takes the most advantage of these assets duration. However, it ignores the risks of waiting until the breakdown of the machine. This effect is shown in Figure 1.4.

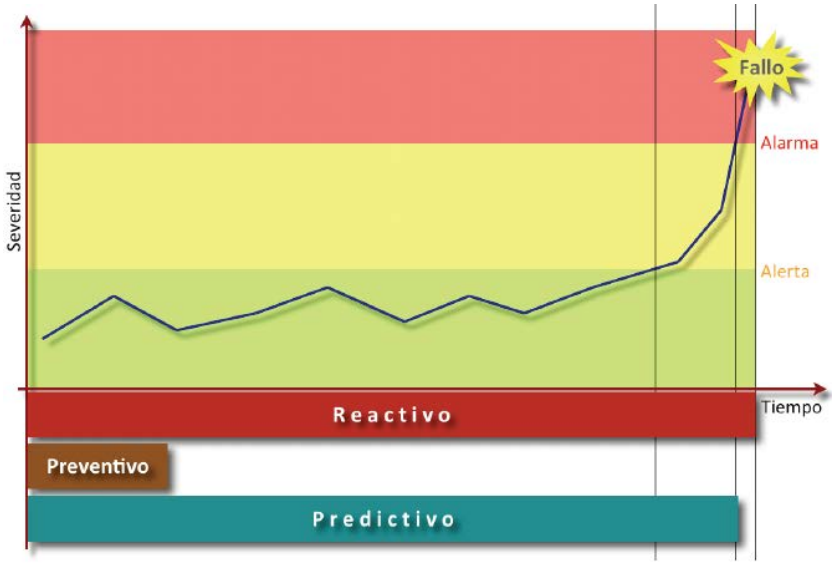

Figure 1. 4 Time comparison between the three main maintenance strategies

A necessity for creating simulation models for rolling elements bearings has appeared in order to get a prediction about the evolution of the defects with a high reduction of costs in maintenance and risks. These models allow implement a width range of faults under different operating conditions and a prediction of when and how problems would appear can be made.

Aim of the investigations

This project has its framework in the investigations of the "Laboratoire des Technologies Innovantes" (LTI), group EESA of the University Picardie <<Jules Verne>> with the direction of Mr Humberto Henao. It is conceived as a part of a bigger investigation about vibration in a complex electro-mechanical system. The ball bearings studied in this project are the points where the rotating movement of the system is hold by fixed supports: ball bearings. The item of the project is, in fact, the modelling and experimental study of faults inside the ball bearings of an electric machine for the surveillance and diagnosis of an electromechanical complex system. The aim of the project of internship is, mainly, take interest over the ball bearings

associated to an asynchronous machine, for the utilisation of a numeric model that might be found in the existing literature. This machine will be adapted itself from the electromagnetic torque transmission to the other parts of the kinematic chain. This model will have to incorporate a minimum of characteristics associated to the inner and outer races as well as to the rolling elements and their cage. This model has been thought to be incorporated to an existing electrical machine model developed in the laboratory itself. The numeric model proposed will be experimentally validated in a test bench that belongs to the laboratory and which is instrumented with several sorts of sensors (mechanic and electromagnetic), under normal conditions and with faults too. The different obtained results will be justified through waveform of the studied signals and their respective frequency spectrum.

General approach and outlines

The non-linearity of ball bearings behaviour makes that the response different from what we can expect and, also, they became very sensitive to the changes on initial conditions. When we try to understand the physical phenomena generated in ball bearings we resort to empirical models (which arise from statistical processes) or mathematical models. Last years, the most used models are those that consider the dynamic effects of the ball bearing, going further from the quasi-static technics widely used around 1960s.

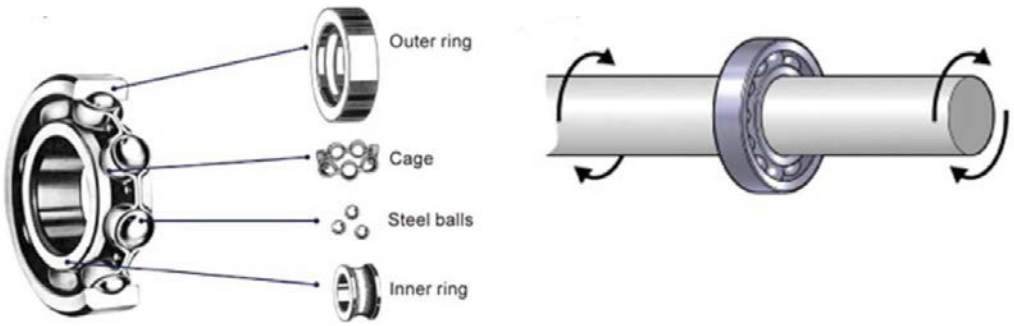

Figure 1. 5 Ball bearing basic elements description

Many kind of models have been developed from those years. Some of them are an analytical model of the bearing with elastohydrodynamic contact considering the parameters of stiffness and damping in the ideal conditions of lubrication presented by Sarabgi [4] or, also, the simplification of the model done by Kennel and Bupara [5] where the cage is only moved in the diameter plane.

Other very relevant works for this project was Darlow et al.[6] and D'Amato et al.[7]. Using the technic of demodulation, the analized the vibrations to diagnostic defects in ball bearings, with more hopeful results than previous studies. Later, McFadden et al.[8] stablished a vibrating model considering the load distribution in the bearing and the presence of a localised fault.

Martin and Honarvar [9] used statistical parameters like skewness and kurtosis to analyze the vibrating signal. Mori et al. [10] applies the Wavelet transformations to predict the spalling fault in bearings.

Danthez et al. [11] introducez a new technic of spectral estimation, based in Fourier Transform, the autocoherent spectrum, which allows an accurate estimation and cancellation of pure tones.

Later, an evolution of diagnostic models that use simultaneously more than one technic at the same time, like Lou et al.(2004), who use both, the wavelet transform and the fuzzy control systems to the diagnosis of bearing faults.

The organisation of this paper is the following:

In the first chapter an introduction around the project is shown with a required description of the importance of the control of bearings in the area of maintenance. An explanation of the aims of the project is given; beginning by the statement of the stage. It finishes with a summary of the articles and people who have already studied around this topic or similar. A little description of this document is shown too.

The second chapter shows a part of the theories that have been used to analyse ball bearings previously. Some of the commonly methods for vibration analyses are listed and explained.

In the third chapter it is explained the performance of a ball bearing with a detailed description of the forces and movements that belongs to a ball bearing.

The fourth chapter shows the equations that represent the model descripted in the previous chapter. The differential equations can be used to create a model.

The numerical method followed is carefully explained in the fifth chapter, with the aim of allowing its future reproduction with the minimum of problems.

In the sixth chapter a conclusion is given after all the explanations.

The references of the seventh chapter list all the projects, thesis and books that have been a source to develop this project.

The eighth chapter owns the annexes that complete the information given during the project. They try to make easier the comprehension the model presented.

2. THEORETICAL FRAMEWORK

Vibration phenomena in machines

We commonly use vibration to see if a machine is “running right” and our own experience sometimes allow us to realise if a machine have a problem. It is natural to associate the condition of a machine with its level of vibration, as we can read in Dennis (1994). Of course, it's natural for machines to vibrate. Even machines in the best of operating condition will have some vibration because of small, minor defects. Therefore, each machine will have a level of vibration that may be regarded as normal or inherent. However, when machinery vibration increases or becomes excessive, some mechanical trouble is usually the reason. Vibration does not increase or become excessive for no reason at all. Something causes it - unbalance, misalignment, worn gears or bearings, looseness, etc.

Human perception of touch and feel is somewhat limited, and there are many common problems such as the early stages of bearing and gear failure that are generally out of the range of human perception. Thus, modern instrumentation for measuring vibration on rotating and reciprocating machinery not only minimizes the need for extensive experience, but makes it possible to detect developing problems that are outside the range of human senses of touch and hearing.

Vibration can be defined as simply the cyclic or oscillating motion of a machine or machine component from its position of rest or balance. It is supposed also that these displacements are relatively small and suitable with elastic deformations that generate tensions much quite smaller-to the elastic limit of the materials. Forces generated within the machine cause vibration. These forces may:

1. Change in direction with time, such as the force generated by a rotating unbalance.

2. Change in amplitude or intensity with time, such as the unbalanced magnetic forces generated in an induction motor due to unequal air gap between the motor armature and stator (field).
3. Result in friction between rotating and stationary machine components in much the same way that friction from a rosined bow causes a violin string to vibrate.
4. Cause impacts, such as gear tooth contacts or the impacts generated by the rolling elements of a bearing passing over flaws in the bearing raceways.
5. Cause randomly generated forces such as flow turbulence in fluid-handling devices such as fans, blowers and pumps; or combustion turbulence in gas turbines or boilers.

Some of the most common machinery problems that cause vibration include:

1. Misalignment of couplings, bearings and gears
2. Unbalance of rotating components
3. Looseness
4. Deterioration of rolling-element bearings
5. Gear wear
6. Rubbing
7. Aerodynamic/hydraulic problems in fans, blowers and pumps
8. Electrical problems (unbalance magnetic forces) in motors
9. Resonance
10. Eccentricity of rotating components such as "V" belt pulleys or gears

The vibrant system model has to represent with the highest exactitude the real vibrating element, characterized by the main mass or inertia matrix, the stiffness or

the stiffness matrix and the damping or the damping matrix and de degrees of freedom (d.o.f.) of the system.

The vibrating analysis measures, from the external parts of the machine, the vibrating signal caused by internal anomalies. The analysis of these signals allows obtaining information of the slow degradation problems. Each kind of fault is associated to certain vibrations, which allow their identification.

With the aim of study vibration components, two domains have been used: temporal domain and frequency domain, which show the amplitude faced with time and frequency respectively. While time domain shows a physical idea of the vibration, it is the frequency domain that is going to allow identifying easily the characteristic frequency components of the vibration.

Velocity and acceleration are the most common parameters of amplitude compared, rather than displacement. Not only the amplitude of the wave is relevant, but also the energy of the fault. In most applications, spike energy alone doesn't sufficiently monitor machine conditions. Concurrently observing it with other vibration parameters (such as acceleration, velocity, or temperature) is helpful to establish useful correlations.

When spike energy increases, it usually means that bearing, gear, or other component problems are developing. It also means that acceleration and velocity trends should be more closely observed for changes; if acceleration readings exceed their allowable vibration limits but velocity readings are still acceptable, vibration spectrum analysis should be performed to confirm the problem. Repairs should be scheduled for a convenient future time.

When velocity, acceleration, and spike energy readings all exceed allowable levels, the observed machine is approaching the end of its useful life. Sometimes, spike energy readings may decrease and, just prior to failure, increase again to excessive values; if

this happens and is seen in time, the machine should be shut down to prevent more avoidable damage.

Generally, the vibrating cause is around mechanical problems like rotating elements imbalance, coupling misalignment, damaged and worn gears, worn bearings, aerodynamic or hydraulic forces, etc.

The vibrating signals can have different frequencies as we can see in the figure 2.1. For example, the diapason has one only frequency, while the combustion engine has two. However, when we see the vibration of more complex systems, the amplitude-time study tends to be insufficient to know how many components and their frequencies the signal have.

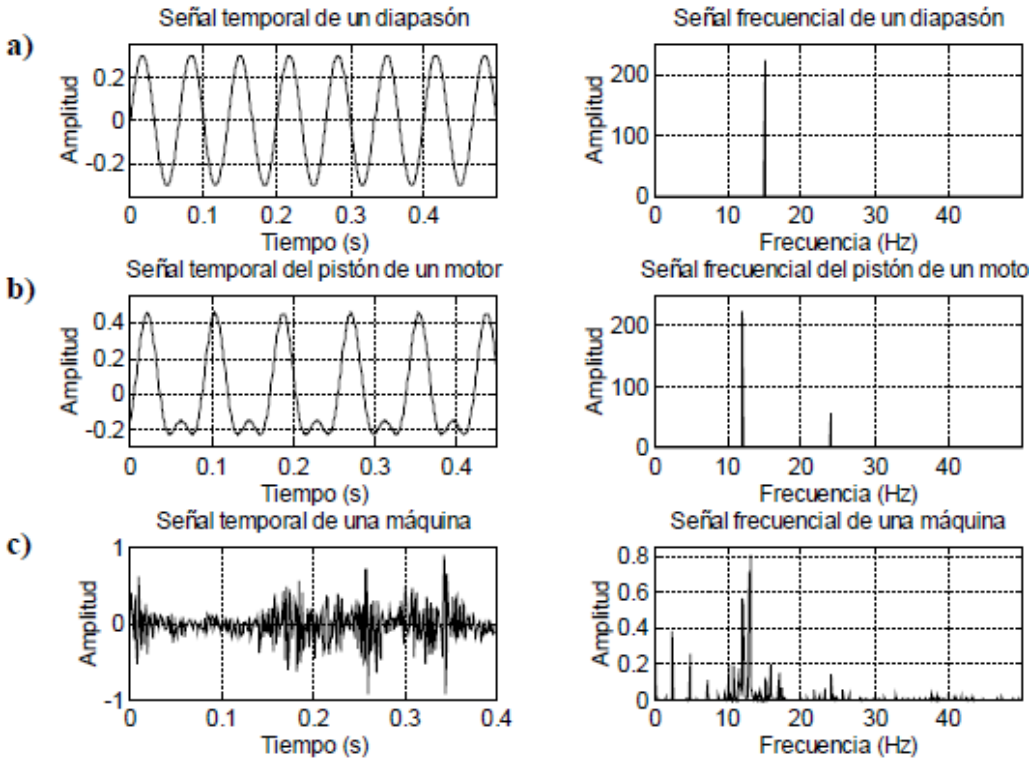

Figure 2. 1 Temporal and frequency representation of the vibration of: a) a diapason, b) a combustion engine and c) a complex machine.

The frequency spectrum of a vibrating signal allows doing an analysis complete without losing any information. The aim of this kind of analysis is decompose a complex signal into more elemental components which let doing an easier study.

Hence, as mechanical rotating systems are associated to cyclic mechanical processes, Fourier Series Method is the tool use to breakdown the signal.

First industrial applications of frequency domain analysis were the analogic spectra analyzers (frequency tuning through bandpass filters), but the algorithm FFT (Fast Transfer Function) is the most extended analyze after digital analyzers became using this FFT algorithm.

In this section will be summarize some of the most important technics and other interesting concepts related with this kind of analysis and that will be applied in this project.

Vibration Signal processing

After measuring a signal or after running a model on the computer, the vibration signal is obtain in amplitude-time mode, and different mathematical methods are used to extract information from them. Some of the methods commonly used in engineer are listed below:

- Fourier Transformation. Fast Fourier Transform (FFT) is the method used here.
- Power Spectral Density (PSD)
- Spectral Envelope
- Spike-Energy
- Wavelet analysis

3. DYNAMIC MODEL OF THE BALL BEARING

Kinematic and Dynamic of the ball bearing

Ball bearings are mainly design to support rotatory parts of a machine, reduce its friction and facilitate smooth rotation of an axis. The ball bearing that we study is going to principally support a radial strength, in the direction of the weight of the machine. Their common components are shown in Figure 3.1. Its basic behavior is an inner race (or ring) that rolls in conjunction with the shaft of the machine, another outer race that is fixed and some rolling elements placed between them. The cage (separator) is an auxiliary component that maintains a constant distance between each ball.

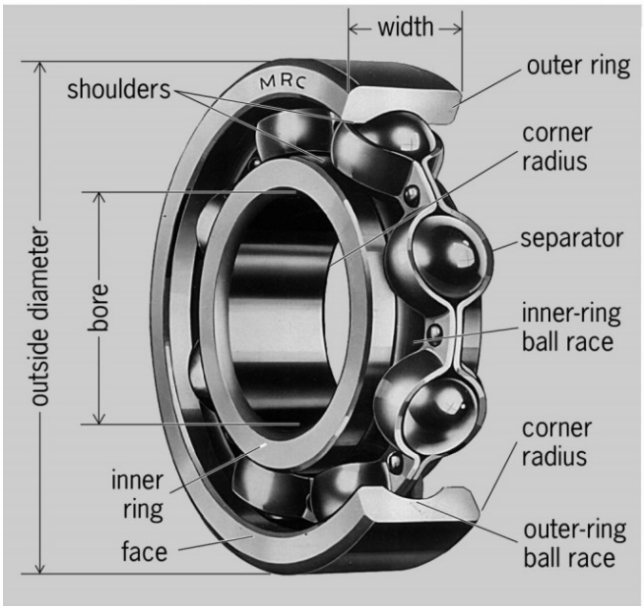

Figure 3. 1 Ball bearing components

To simplify the kinematic study, the movement will be considered the plane perpendicular to the axis of the shaft. The rolling movement of the shaft and the inner race will generate the movement of the balls and their cage. The rolling elements have

two movements, rotatory velocity of the ball upon itself, and the rotatory velocity around the shaft, which can be seen as follows.

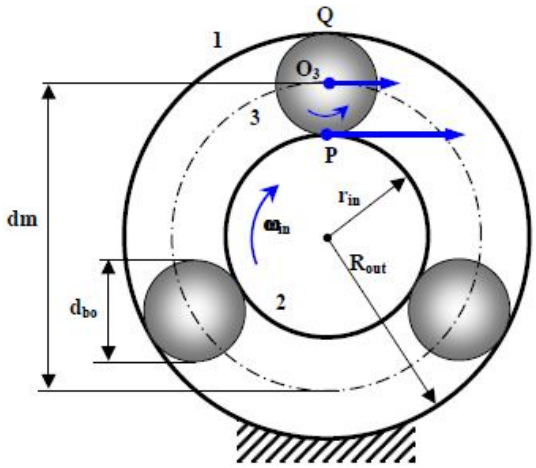

Figure 3. 2 Kinematic of the ball bearing

For this model it is consider that there is no slippage, that is to say there are rolling movements between the balls and the races. Therefore, kinematic equations can be obtained directly from its geometry.

Likewise, a dynamic in the model can be shown as follows. The only load applied is in radial direction, and here it is shown only the main load, in the vertical axis.

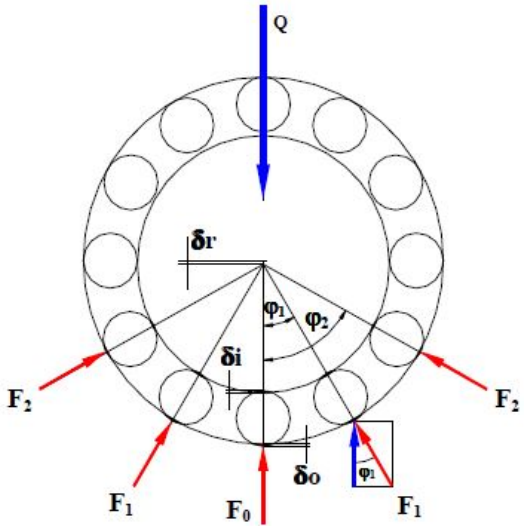

Figure 3. 3 Dynamic of the ball bearing

The generic relative displacement-load relation in a ball bearing can be expressed like this equation:

$$\delta_n = K_n \cdot Q^T \qquad (3.1)$$

Where:

- Q is the total load applied on the ball bearing.
- T is a coefficient which value is 2/3 in the cases of ball bearings where the contact point between different parts is a point.
- Kn is a coefficient that depends on the kind of bearing.

The total deformation in the direction of the most loaded element shown in Figure 3.3, is given by:

$$\delta = \delta_{\text{in}} + \delta_{\text{out}} \qquad (3.2)$$

Where:

- δ_{in} is the deformation between the rolling element and the inner race.
- δ_{out} is the deformation between the rolling element and the outer race.

It is useful to say that this deformation will be named also displacement of the position of the centre of the inner race. This is normal because its displacement appears in the same direction and quantity of the deformation, the sum of all the deformations.

In this project, the parameters used are the ones proposed in the thesis [1], which make reference to a ball bearing SKF 6206. So, through a method explained there, stiffness constants can be calculated with the geometrical parameters of the ball bearing used. The results achieved and used in this model for the stiffness constants are:

$$C_{in} = 905890 \ \frac{N}{mm^{3/2}}$$

$$C_{out} = 937318 \ \frac{N}{mm^{3/2}}$$

The contact ball-inner race and ball-outer race are produced simultaneously. Therefore, we can calculate an equivalent stiffness constant value, C_{eq} , considering that the angle of the forces of both contacts are near to zero, $\beta = 0$. Then, deformations will be calculated in the direction of the vector $\vec{r_i}$, considering the previous analogy. It is shown in Figure 3.4.

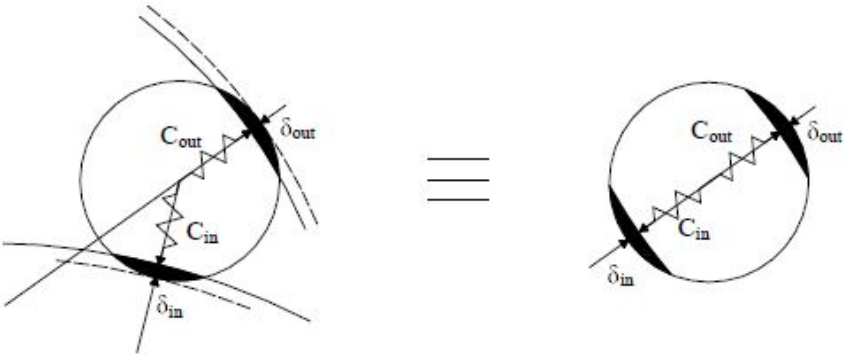

Figure 3. 4 Contact ball with inner and outer races

In this way, both springs are in series connection and the equivalent stiffness constant can be calculated as follows:

$$\frac{1}{C_{eq}^{\ 2/3}} = \frac{1}{C_{in}^{\ 2/3}} + \frac{1}{C_{out}^{\ 2/3}} \qquad (3.3)$$

Replacing in this equation the previous values of C_{in} and C_{out}, we obtain a value for this ball bearing of:

$$C_{eq} = 325757 \ \frac{N}{mm^{3/2}}$$

The force that appears between the ball and both inner and outer races can be calculated with this relation:

$$F_i = C_{eq} . \delta_i^{\ 3/2} \qquad (3.4)$$

It is important to see that here there is a little difference with the source of information [1] of this equation. In the model analysed here, this equation that represents the forces. In this model C_{eq} will be the only value of the stiffness value.

Therefore, the force that we will see is the result of both, the inner race and the outer race contact with the ball.

Model of 2 d.o.f.

Cartesian equations

The model under study considers that the radial distance from the centre of the balls to the centre of the outer race is constant. The outer race is locked and without movement, while the inner race is settled to the shaft of the motor rolling with a constant angular velocity ω_s. The centre of the outer race will be the origin of polar coordinates.

In order to guess the vibratory characteristics, the model can be considered as a damping-spring-mass-mounted system. The elastic deformation between the races and the rolling elements, in this model, presents a relation force - non-linear deformation that can be obtained through Hertzian theory. It will be then described by the constants of damping coefficient (D), stiffness constant (C_{eq}) and the mass of the shaft (m_s), inner race (m_{in}) and balls (m_b).

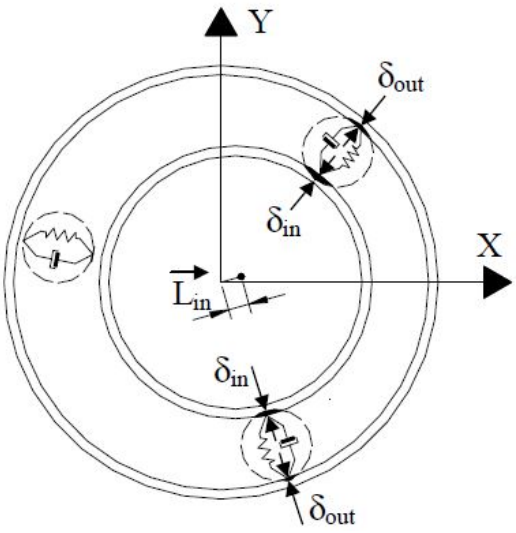

Figure 3. 5 Spring-mass model of the ball bearing

In the centre of the outer race will be the reference system origin. The positions of the centre of the inner race and the centre of the balls will be named as $\overrightarrow{L_{in}}$ and $\vec{r_i}$, respectively. The position of the ball from the centre of the inner race would be $\overrightarrow{\rho_i}$. Some hypotheses have been considered in this simplified model:

- Deformations follow the Hertzian theory.
- Balls and rotor movements are in the same plane.
- Angular velocity of the cage is constant.
- Balls do not have angular rotatory velocity.
- All components are rigid.
- There is no slippage between the balls and the surfaces where the movement is produced.
- The cage keeps all balls at equal intervals, so there is no interaction between balls.
- The distance between the centres of the balls to the centre of the outer race is constant (27mm in this model).
- Despite the deformation ball – inner race has the direction of the line $O_b - O_{in}$, as the angle β is very little, we can consider that this deformation is in the line $O - O_b$. Because of the same reaction, we will consider that the reaction $F_i$of the ball to the inner race has the same direction $O - O_b$, and their components are calculated through the angle α_i of each ball.

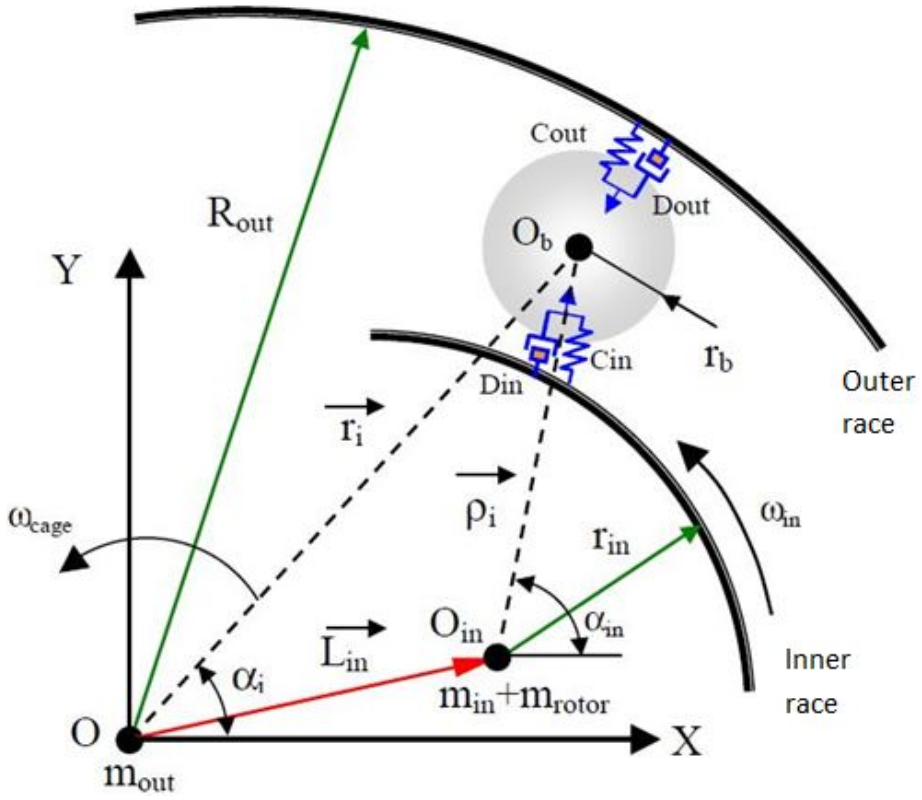

Figure 3. 6 Proposed Ball bearing model

In a model of two degrees of freedom (2dof) the movement equations are obtained from the application of Newton equations to the diagram of the ensemble rotor – inner ring. The following figure:

- Weight of the inner ring and weight of the rotor, $((m_{in} + m_{rotor}) \cdot g$
- An extern force, Fe_x, Fe_y
- A radial force due to unbalance in the rotor, Fu
- The forces due to the elasticity of the contact, Fin_x^i, Fin_y^i.

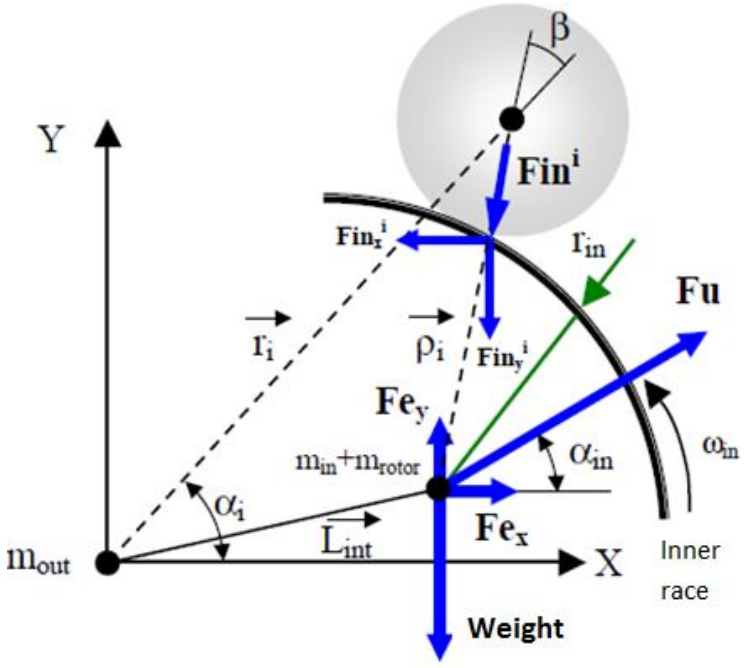

Figure 3. 7 Diagram of forces of the ball bearing

The Newtown's Second Law, in normal coordinates, is as follows:

$$(m_{in} + m_{rotor}) \cdot \ddot{x} = \sum F_x \quad ; \quad (m_{in} + m_{rotor}) \cdot \ddot{y} = \sum F_y \tag{3.5}$$

Simplifying the value of the angle $\beta \approx 0$, we can get the equations for both axes:

In the x direction:

$$(m_{in} + m_{rotor}) \cdot \ddot{x} = F_{ex} + F_u \cdot \cos(\alpha_i) - \sum_{i=1}^{n_b} F_{in_i} \cdot \cos(\alpha_i) \tag{3.6}$$

In the y direction:

$$(m_{in} + m_{rotor}) \cdot \ddot{y} = F_{ey} + F_u \cdot \sin(\alpha_i) - \sum_{i=1}^{n_b} F_{in_i} \cdot \sin(\alpha_i) - (m_{in} + m_{rotor}) \cdot g \tag{3.7}$$

The forces of the balls are calculated through the Herztian theory shown in the equation 3.4, where the value of the deformation is calculated as the displacement of the inner race:

$$\begin{matrix} \delta_i = x_{in} \cdot \cos(\alpha_i) + y_{in} \cdot \sin(\alpha_i) & \text{if } \delta_i \geq 0 \\ \delta_i = 0 & \text{if } \delta_i < 0 \end{matrix} \quad (3.8)$$

Differential equations of the movement with 2 d.o.f. model

The equations 3.9 and 3.10 represent the differential equations of the movement of the rotor, applying the Newton's Second Law, when the ball bearing has 3 or 9 balls. So, the value of n_b is changed by these values for each one of the models. In the x direction:

$$(m_{in} + m_{rotor}) \cdot \ddot{x} = F_{ex} + F_u \cdot \cos(\alpha_i) - \sum_{i=1}^{n_b} F_{in_i} \cdot \cos(\alpha_i) \quad (3.9)$$

And in the y direction:

$$(m_{in} + m_{rotor}) \cdot \ddot{y} = F_{ey} + F_u \cdot \sin(\alpha_i) - \sum_{i=1}^{n_b} F_{in_i} \cdot \sin(\alpha_i) - (m_{in} + m_{rotor}) \cdot g \quad (3.10)$$

It is important to say that the system of unities used is the international system. Therefore, each terminus have the same unites which, in this case, they are $\boldsymbol{kg \cdot m/s^2}$, or, which is the same, $\boldsymbol{N}$(newtons).

Model of 2+Z d.o.f.

In this section the equations of a model of 2+Z d.o.f will be shown, for the same ball bearing that was introduced above. The Z d.o.f. added to the model belongs to the number of balls included in the ball bearing model. Hence, the ball bearing model with 3 ball presents 5 d.o.f and the model with 9 ball 11 d.o.f.

Each d.o.f. added comes from the the equation that represent the balance of forces of each ball. The 2+Z equations are, as is explained in [1], the same as in the 2 d.o.f plus the equations of the balls. So, the equations that are added to the model are, for 3 balls, as follows:

$$(m_{bo}) \cdot \ddot{r_1} = C_{in} \cdot {\delta_{in_1}}^{3/2} - C_{out} \cdot {\delta_{out_1}}^{3/2} - D_{in} \cdot \dot{r}_1 \cdot \Gamma_{in} - D_{out} \cdot \dot{r}_1 \cdot \Gamma_{out} + \ldots \quad (3.11)$$
$$\ldots + m_{bo} \cdot r_1 \cdot {\dot{\alpha}_{in}}^2 - m_{bo} \cdot g \cdot \sin(\alpha_1)$$

$$(m_{bo}) \cdot \ddot{r_2} = C_{in} \cdot {\delta_{in_2}}^{3/2} - C_{out} \cdot {\delta_{out_2}}^{3/2} - D_{in} \cdot \dot{r}_2 \cdot \Gamma_{in} - D_{out} \cdot \dot{r}_2 \cdot \Gamma_{out} + \ldots \quad (3.12)$$
$$\ldots + m_{bo} \cdot r_2 \cdot {\dot{\alpha}_{in}}^2 - m_{bo} \cdot g \cdot \sin(\alpha_2)$$

$$(m_{bo}) \cdot \ddot{r_3} = C_{in} \cdot {\delta_{in_3}}^{3/2} - C_{out} \cdot {\delta_{out_3}}^{3/2} - D_{in} \cdot \dot{r}_3 \cdot \Gamma_{in} - D_{out} \cdot \dot{r}_3 \cdot \Gamma_{out} + \ldots \quad (3.13)$$
$$\ldots + m_{bo} \cdot r_3 \cdot {\dot{\alpha}_{in}}^2 - m_{bo} \cdot g \cdot \sin(\alpha_3)$$

Where:

$$\Gamma_{in} = 0 \quad \text{if } \delta_{in} < 0 \quad ; \quad \Gamma_{in} = 1 \quad \text{if } \delta_{in} \geq 0 \quad (3.14)$$
$$\Gamma_{out} = 0 \quad \text{if } \delta_{out} \geq 0 \quad ; \quad \Gamma_{out} = 1 \quad \text{if } \delta_{out} \geq 0$$

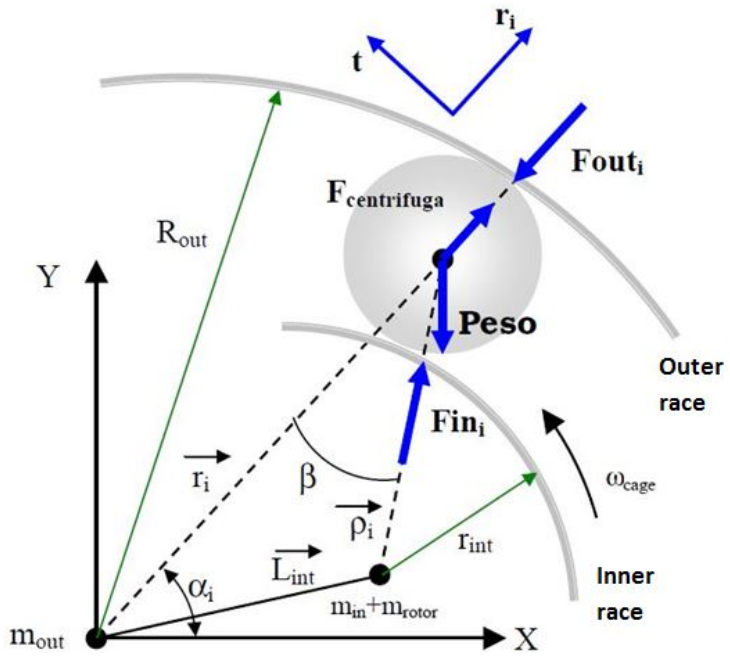

Figure 3. 8 Diagram of forces (2+Z d.o.f.)

The diagram of forces is the same as the one used before, as well as the approximations. The force F_{in} that appears in each ball can be considered to be applied in the r_i axis due to the approach $\beta \approx 0$.

4. NUMERICAL SIMULATION METHODOLOGY

In this section the equations of the model that have been explained before will be implemented. The values for the constants will be taken from [1] so the results can be compared. The ball bearing study is SKF 6206 which geometry and physical properties are described in the following pages.

The program used for doing these calculations is Matlab and Simulink. As they are differential equations, the first idea was working in a sheet o Matlab and solving the model using the method ode45. Despite the difficulty of the model due to its non-linearity, a mathematical method was applied to solve it. However, it was very slow and complicated to develop later so the model was implemented in Simulink. Here, all the blocks will be shown and explained, so there are not further mistakes applying this model.

These simulations tools have been frequently used for the vibration analysis, and even more for simulate mechanical systems like ball bearings. They are also used to simulate under different kind of working conditions.

Simulink is a tool that works with blocks, which simplifies the edition of the equations as well as its comprehension. The values of the constants introduced in Simulink can be defined. These values have been written in a sheet called “Data_bearing_2dof.m”, that can be found in the annexes. Its execution is required before running Simulink. The results can also be sent to the Workspace through the block “simout” so they can receive a better analyse.

Any kind of graphic, like temporary or frequency domain graphics can be shown in both places. Here, usually, the temporary graphics will be in a Scope while the frequency domain ones will be shown through Matlab, where the FFT is applied.

Model of 2 d.o.f. with 3 balls

In this section the integration of (3.9) and (3.10) differential equations into Simulink is explained. The values of the constants that will not change and are defined in Data_bearing_2dof.m are:

Damping coefficient (experimental [1]) $D = 0.0158\ {}^{N \cdot s}/_{mm}$

Equivalent stiffness constant: $C_{eq} = 325757\ {}^{N}/_{mm^{3}/_{2}}$

Geometry: Ball diameter: $Db = 9.5$ mm

Cage diameter: $Dc = 46$ mm

The structure of the Simulink model is as follows:

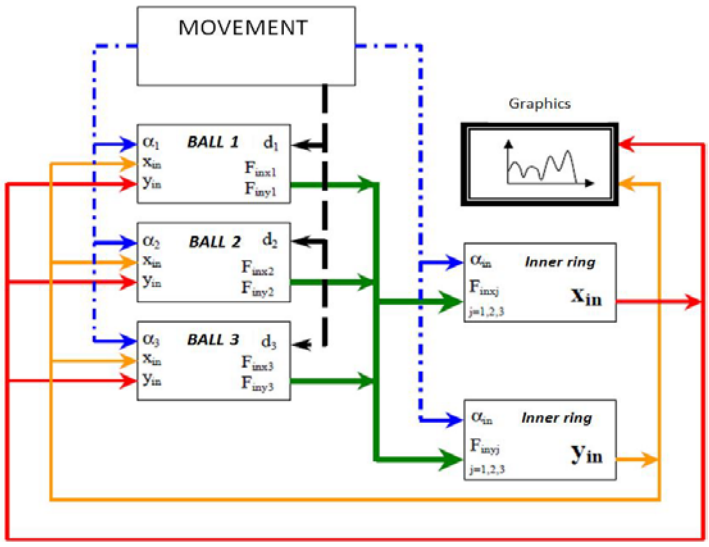

Figure 4. 1 Structure of the Simulink model

This figure is a representation of the real model implemented in Simulink which blocks are shown below as they are seen in the program:

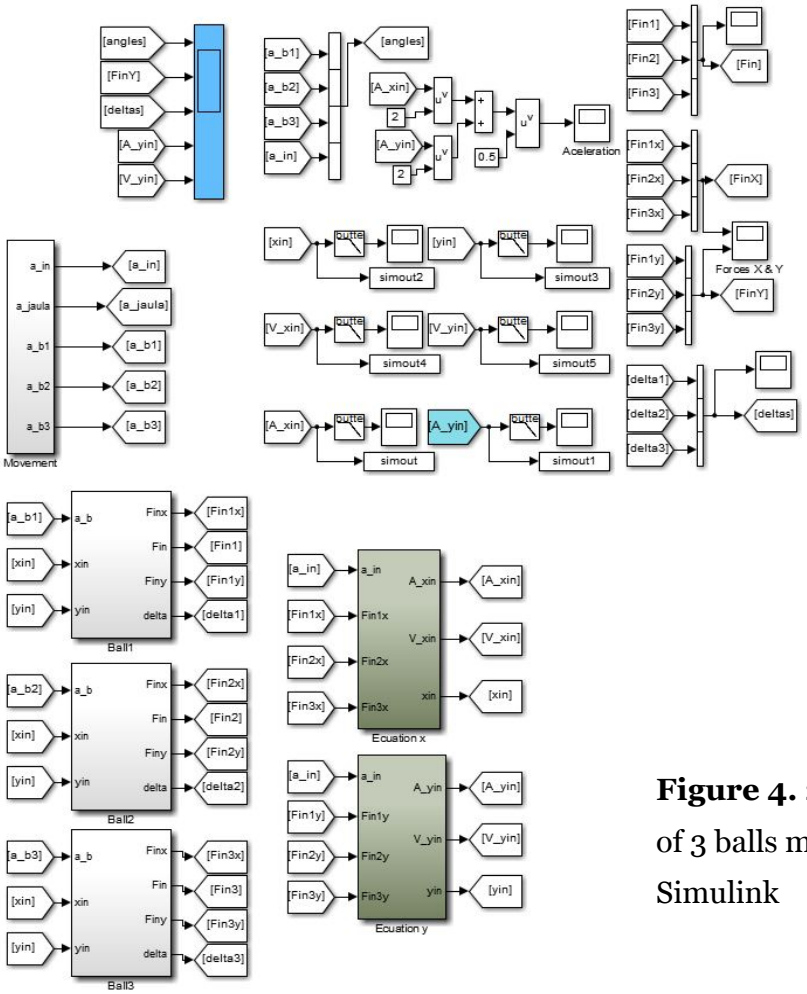

Figure 4. 2 Blocks of 3 balls model in Simulink

We can see in figure 4.1 the blocks that are required to define the model. Their characteristics and functions are explained below:

1. **Movement** block. Inside this block all the parameters as angles as velocities are defined.

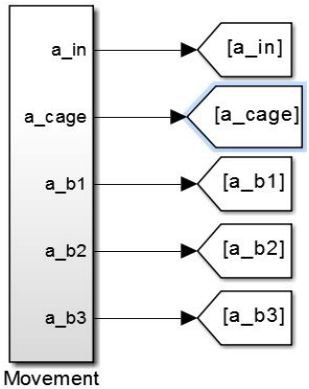

Figure 4. 3 Movement block of 3 balls model

Inside this job, angles are defined as follows:

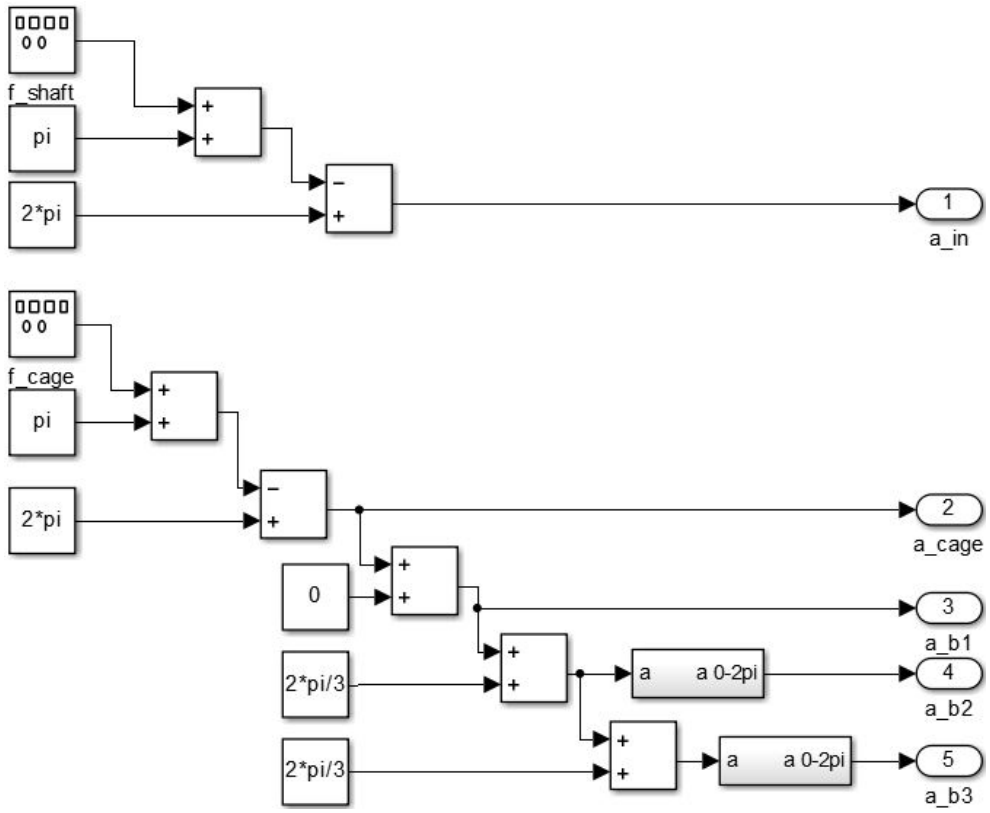

Figure 4. 4 Inside of movement block of 3 balls model

The frequencies of the block, f_shaft and f_cage are defined in the file Data_bearing_2dof.m.

The angles 2*pi/3 represent the gap between each consecutive ball.

The sub block that has the letters “a-->a 0-2pi” change the angle into a value between 0 and 2 π rad, but does not affect the result. Its interior is this:

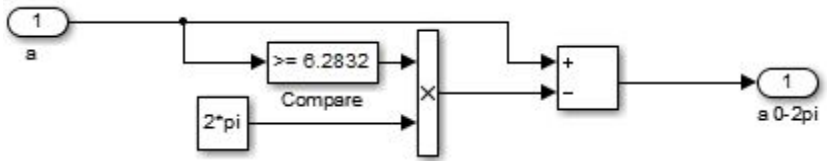

Figure 4. 5 Transformation to 0-2pi rad block

2. **Ball** block. Each one of these block define one terminus of the sum term of the equations (3.9) and (3.10). We can see them below:

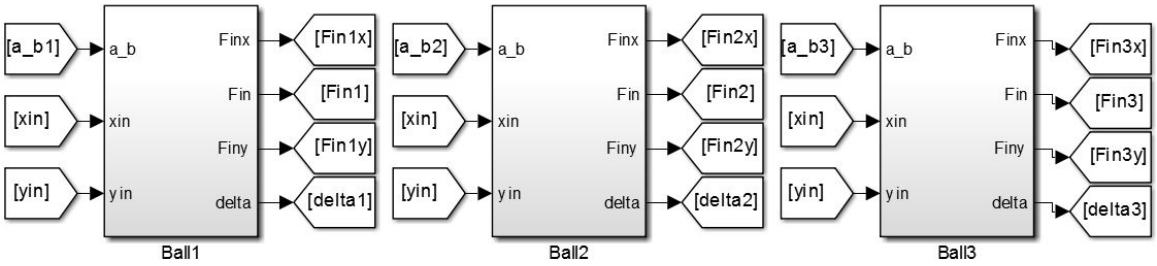

Figure 4. 6 Ball blocks of 3 balls model in Simulink

The interior of each block is exactly the same and it is as follows:

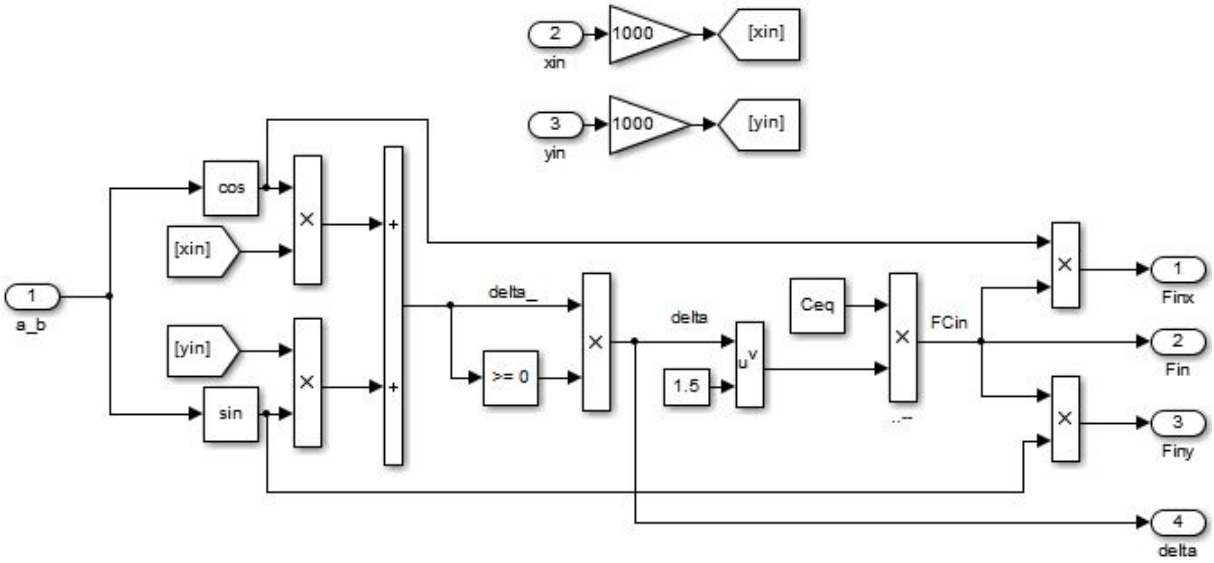

Figure 4. 7 Inside of ball blocks

Here, the terminus 1000 is different from the original model of [1], so an explanation is required:

This ball block represents the terminus $F_{in_i} \cdot \cos(\alpha_i)$ and $F_{in_i} \cdot \sin(\alpha_i)$ of the differential equations (3.9) and (3.10). As it was said in the previous section, the unities of each terminus are newton.

In the one hand, the constant C_{eq} is expressed in $N/mm^{3/2}$, so the value of $\delta_i^{3/2}$ has to be expressed in $mm^{3/2}$. Or, in the same way, δ_i is expressed in mm. If we want to

express δ_i in mm, from the equation (3.8), the unities of the position of the inner ring (x_{in}, y_{in}) have to be introduced in mm too.

On the other hand, the values of the position of the inner race (x_{in}, y_{in}) are calculated in the block of the inner ring, and its output is in m, because the terminus of the aceleration in the equation have to be in m/s^2.

After this explanation, the model presented here probably has this difference from the models shown in the previous bibliography. The results are compared in the following section and they are quite similar though.

3. **Inner ring** block, x_{in} and y_{in}. These two blocks are quite similar and the only difference is in the terminus added to the equation in y axis because of the gravity. They are seen in Simulink as it is shown in figures 4.8 and 4.9.

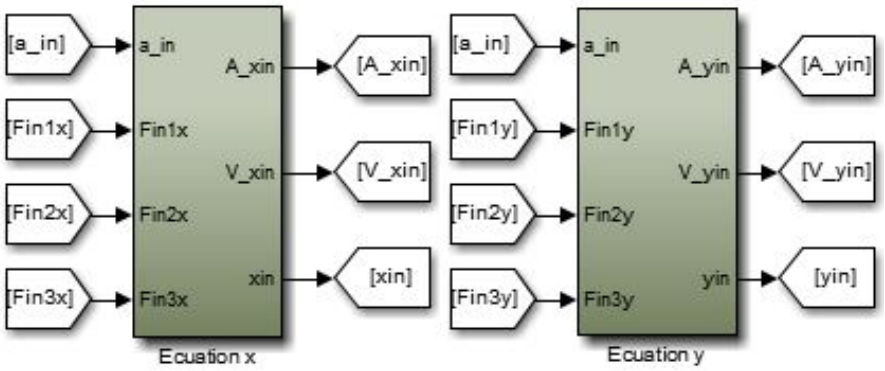

Figure 4. 8 Inner ring blocks of 3 balls model in Simulink

According to the inputs of the figure 4.8 , the three forces (six values) come from the ball blocks, and the inner race angle, a_in, comes from the movement block. Then, the outputs are the signals that we want to measure. Only the position, x_in and y_in are used again in the ball blocks.

Looking inside the inner ring blocks, we can see these distributions:

In the X axis:

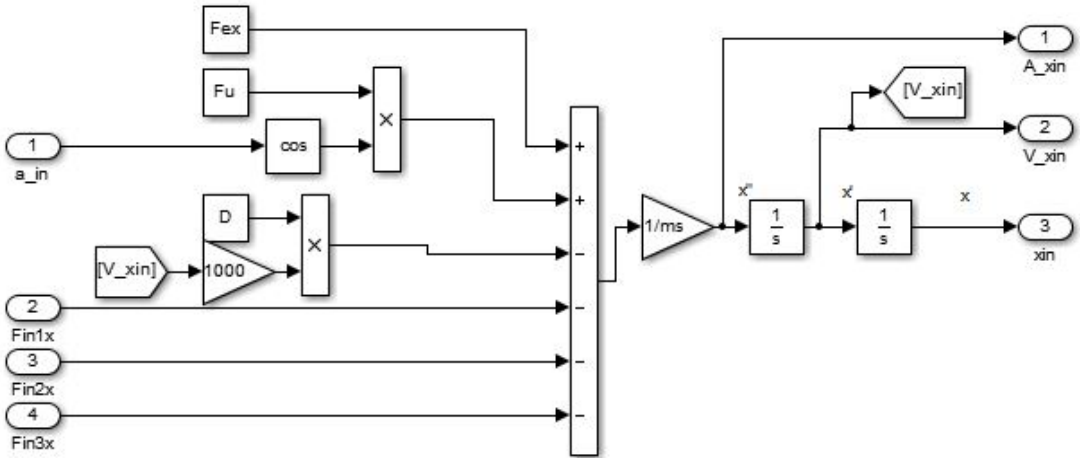

Figure 4. 9 Inside Inner ring blocks of 3 balls model in Simulink - X axis

In the Y axis

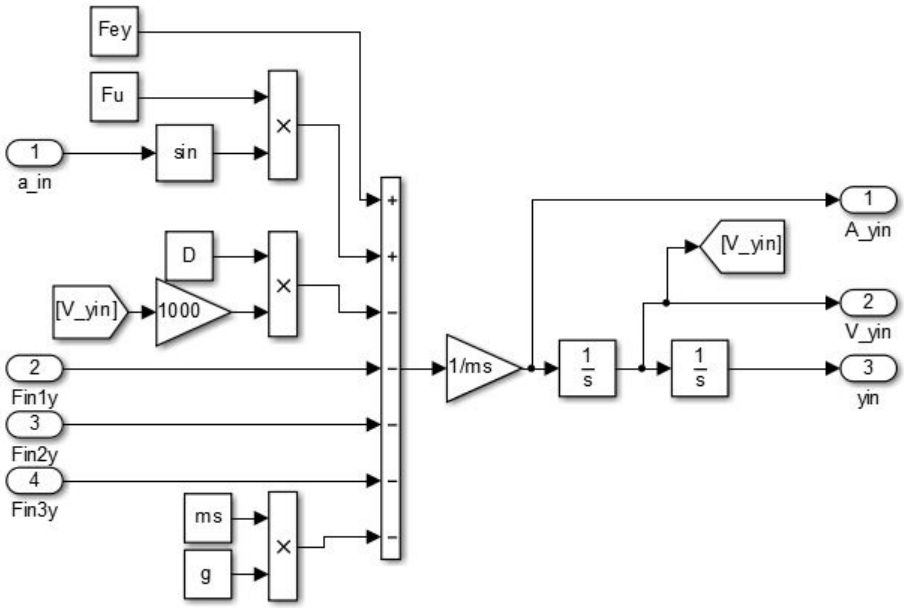

Figure 4. 10 Inside Inner ring blocks of 3 balls model in Simulink - Y axis

Here there are important things that could create confusion. Firstly, the terminus of the damping coefficient *D* doesn't appear in the differential equations of motion. This

terminus would go with a first derivate and the mathematical problem become more difficult and long. However, in iterative process programs like Simulink this is not a problem.

Secondly, as the terminus doesn't come in the equations, its sign has been taken negative because it works as a damper, trying to reduce the variations of velocity of the inner ring.

Thirdly, a factor of 1000 has been incorporated to the model. It has been required after an analysis similar to the one done previously in the ball block with the value of the position. As the factor D is expressed in $N \cdot s/mm$, the value of the velocity has to be introduced in mm/s. And the output of the sinal of the velocity is in m/s, so a factor of 1000 is required.

4. **Graphics** block. In spite of considering this as a block, in the model they have been drawn separately. Here most relevant values have been represented.

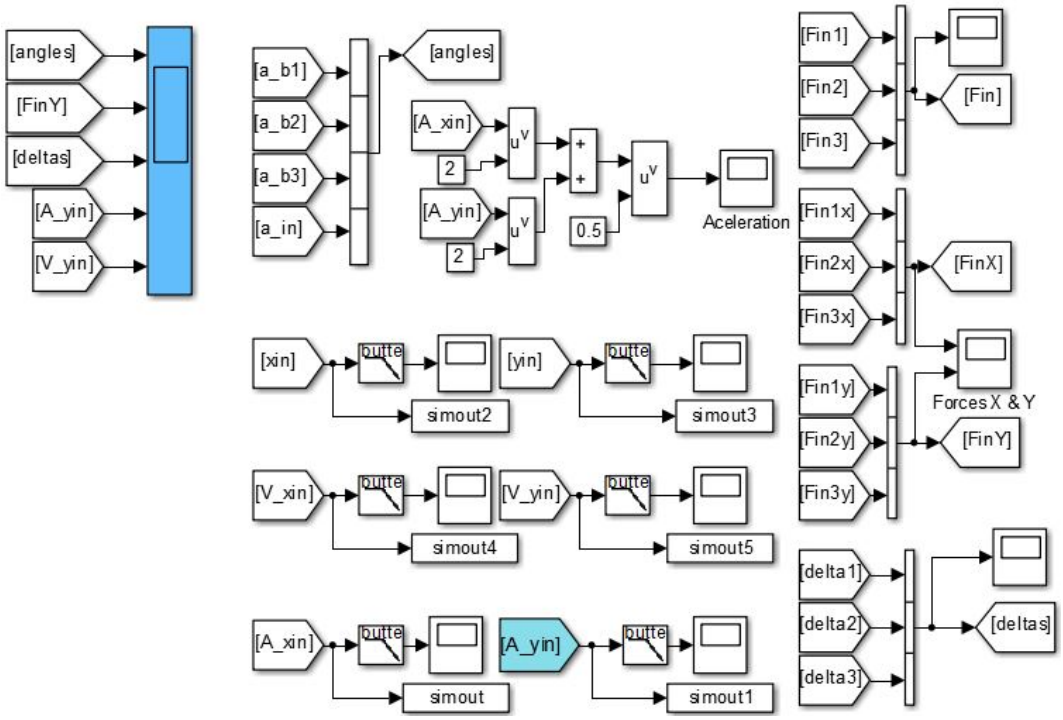

Figure 4. 11 Graphics block

For the analysis of the model, the vertical axis has been the most represented because it supports the weight of the motor. The outputs in the values of the position coordinates allow having the results as a vector in the workspace. Then, a Fast Fourier Transformation is made to show an analysis in frequency.

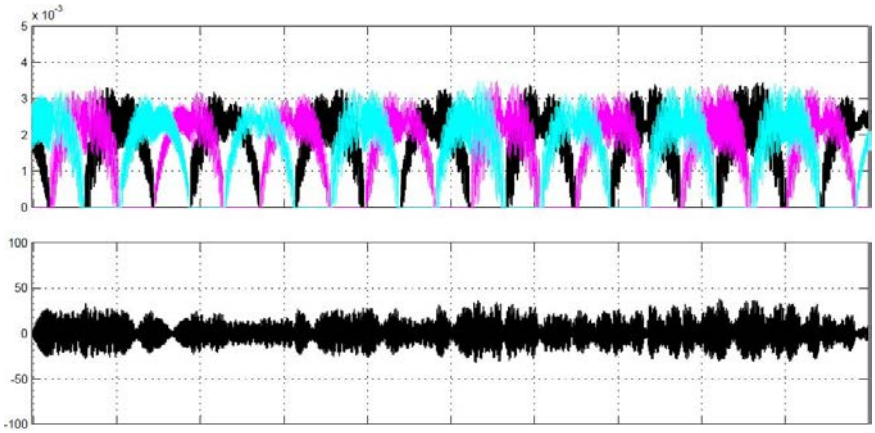

Figure 4. 12 Example of graphic results. ForcesY(N),deltas(m),Ay (m/s2)

Model of 2 d.o.f with 9 balls

The simulation model for 9 balls is very similar for the one of 3 balls. Only some changes are necessaries. The equations represented are the same, (3.9) and (3.10), with the value $n_b = 9$. The blocks of diagram in Simulink are as follows:

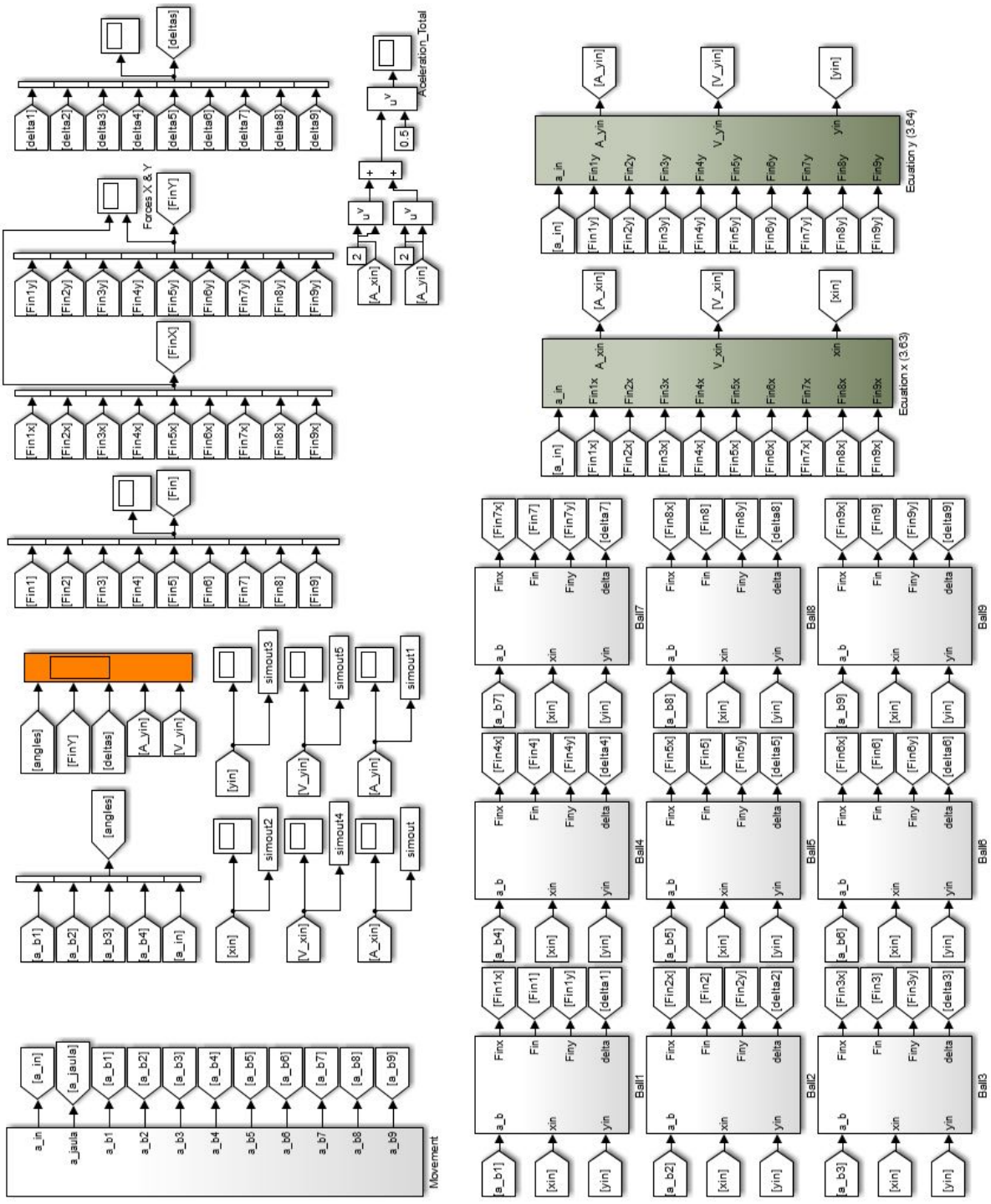

Figure 4. 13 Blocks of 9 balls model in Simulink

1. **Movement** block. The angles defined here have smaller gaps between then, but the performance is just the same. The diagram within this block is as follows:

The angle gap between each consecutive ball is $\frac{2\pi}{9} = 40°$.

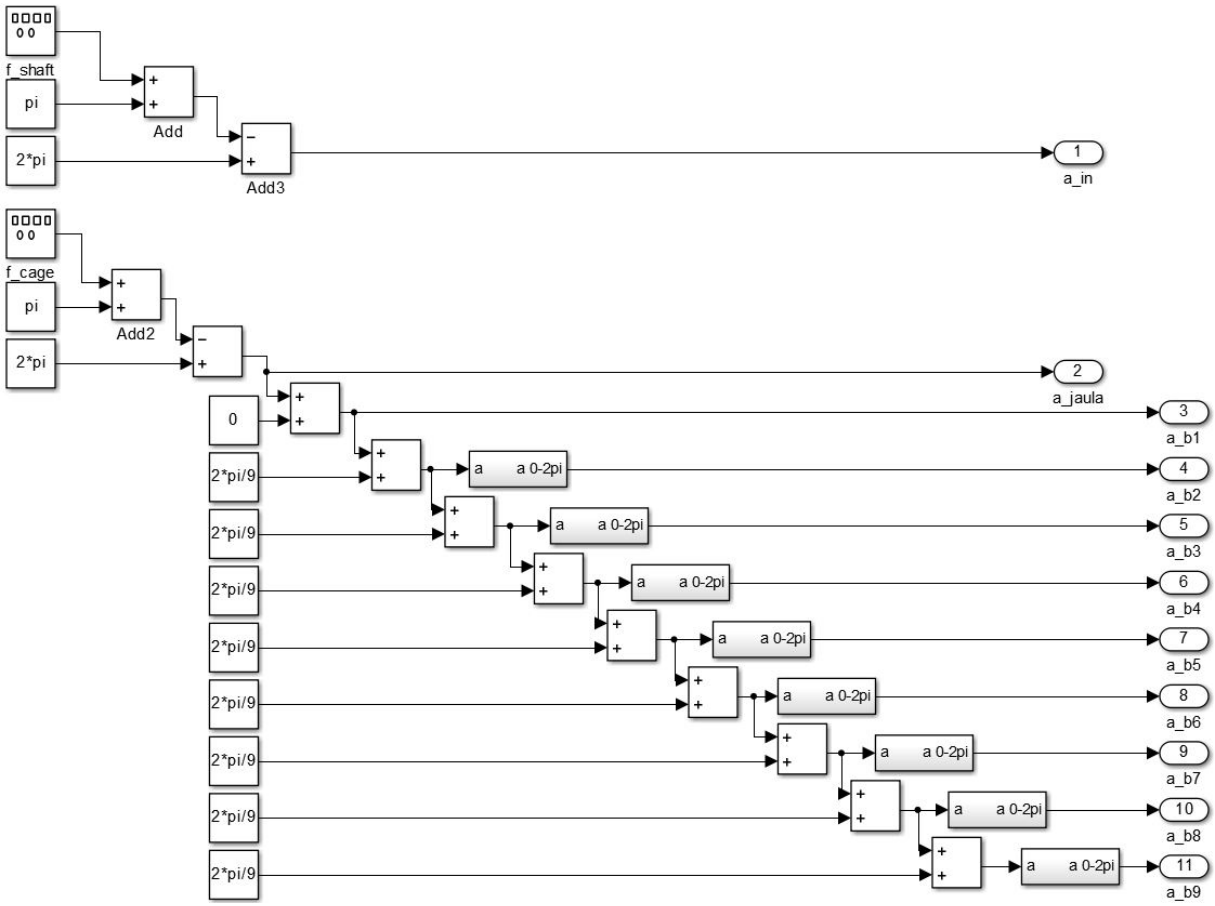

Figure 4. 14 Inside of movement block of 9 balls model

2. **Ball** block. Here the block is completely the same. It is not required to make any change because it works only with the angle of the ball and the position of the inner ring, the same as in 3 balls model.

3. **Inner ring** block, x_{in} and y_{in}. Within these blocks the size of the diagram is bigger because it has to add each one of the 9 terms of the balls in the equations, but the performance is the same. It is as follows:

   Equation in X axis:

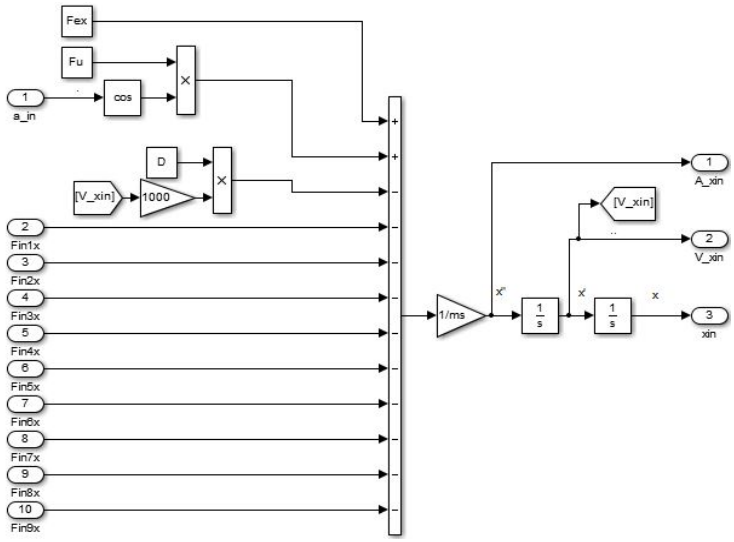

Figure 4. 15 Inside Inner ring blocks of 9 balls model in Simulink - X axis

Equation in Y axis:

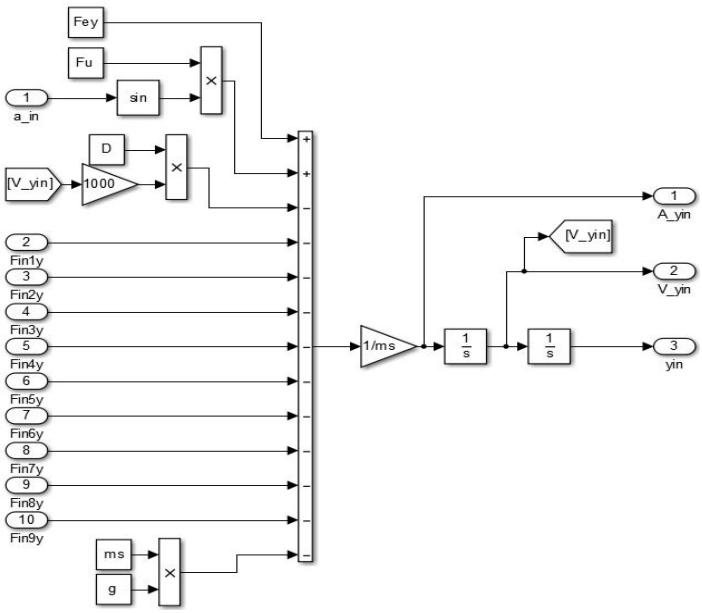

Figure 4. 16 Inside Inner ring blocks of 9 balls model in Simulink - Y axis

4. **Graphics block**. The graphics showed here are equivalents to those of 3 balls model.

5. NUMERIC MODEL RESULTS

In this section, results from the models of 3 and 9 balls are showed and explanations about their coherence with normal results are given. Those graphics will be also compared with the experimental results given in [1] so this model has been able to be validated.

The simulations have been done with a fixed step size of 10^-5 with solver method ode3 (Bogacki-Shampine) in both cases. This size of the step allowed having a reliable response and the executing time is not too long. The alternative of variable-step gave wrong results or even divergent.

Despite both models have consistent results, 9 balls model will be more used because it is more representative of the real ball bearing.

Model of 2 d.o.f. with 3 balls

In the simulations of this model we can see a transitional period of around 0.1-1s which depends on the original conditions. The steady state is not very clear though, and that is because of the high frequency noise that comes from the model.

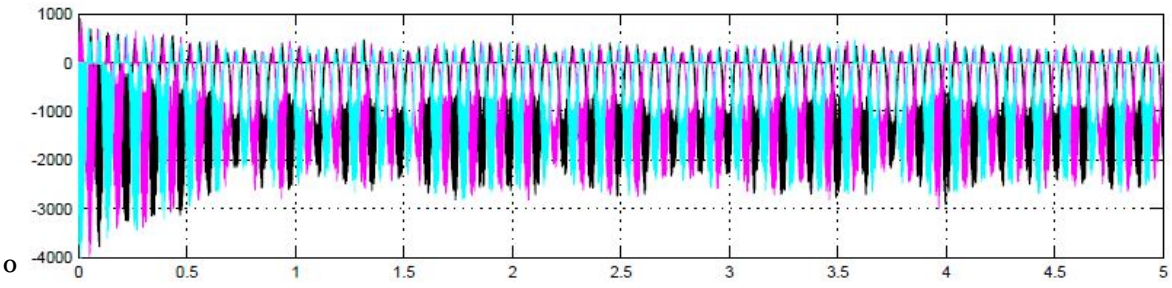

Figure 5. 1 Transitional period of time for forces in the 3 ball model.
Graphic of Y axis Forces (N) – time (s)

Each one of the forces represented in the figure 5.1 is represented by one colour, so its cyclic performance can be seen. The figure 5.2 shows the most important signals that we can obtain in the model. As it was said before, here are represented the Y axis results, but X axis results have similar shapes with different values depending especially on the value of the extern force applied. The five graphics shown in this figure represents: the angle of the balls and the shaft, the forces that appears over the balls (that is why it is negative), the deformation or the displacement (delta) of the balls generated by the forces, the acceleration of the inner race and its velocity. The two last results that appear here appear to have too big amplitudes, but they are not representative of the reality. The reason is the high amplitude that appears at high frequencies is bigger than the amplitude of the main vibration, so it is impossible to see anything.

3 balls model with load of ms=5kg, Fex_y=2000N, Fex_x=0; Fu=0 and a frequency fs=20 Hz.

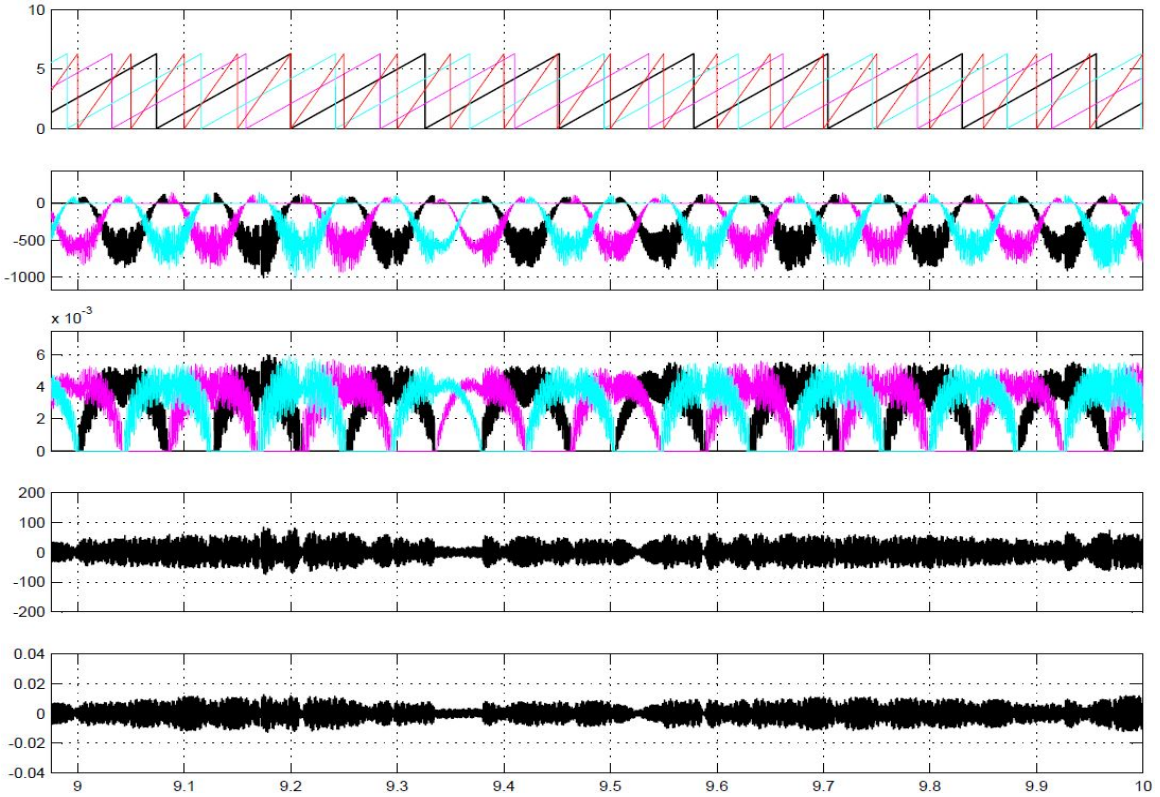

Figure 5. 2 Temporal response of Angles(rad), Forces(N), delta(mm), Acceleration (m/s^2), velocity (m/s) for Y axis

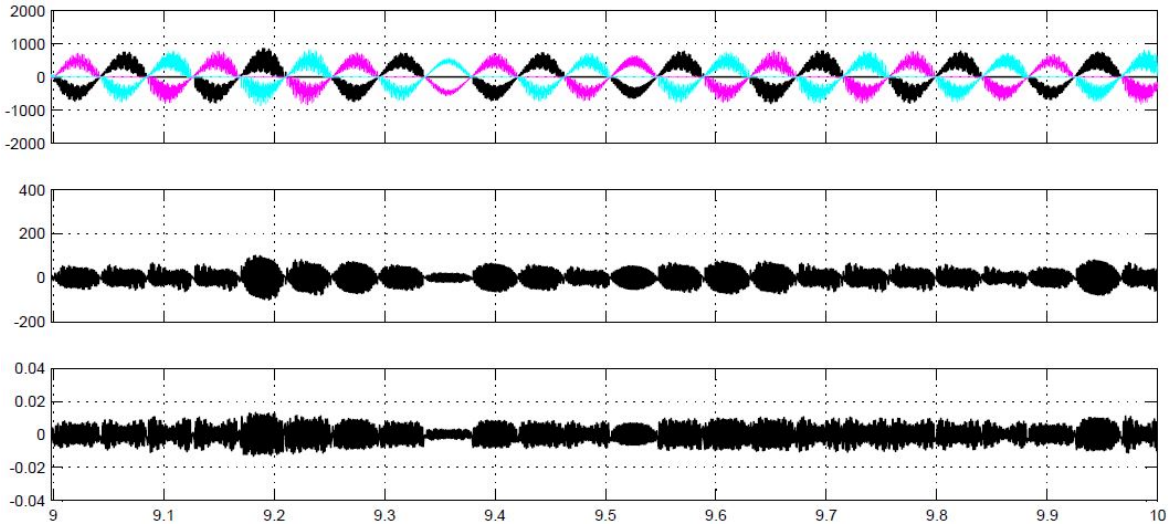

Figure 5. 3 Temporal response of Forces (N), Acceleration (m/s^2), velocity for X axis

In order to obtain some information from the vibration signal (acceleration), a filter was set before the scope of the acceleration for the figure 5.4. In spite of the fact that the verification of this result has not been checked, it is useful to say that the amplitude of the low frequencies of the signals is not as shows the previous figure. Here is presented a signal after a filter of Simulink, which filter for frequencies higher than 30Hz..

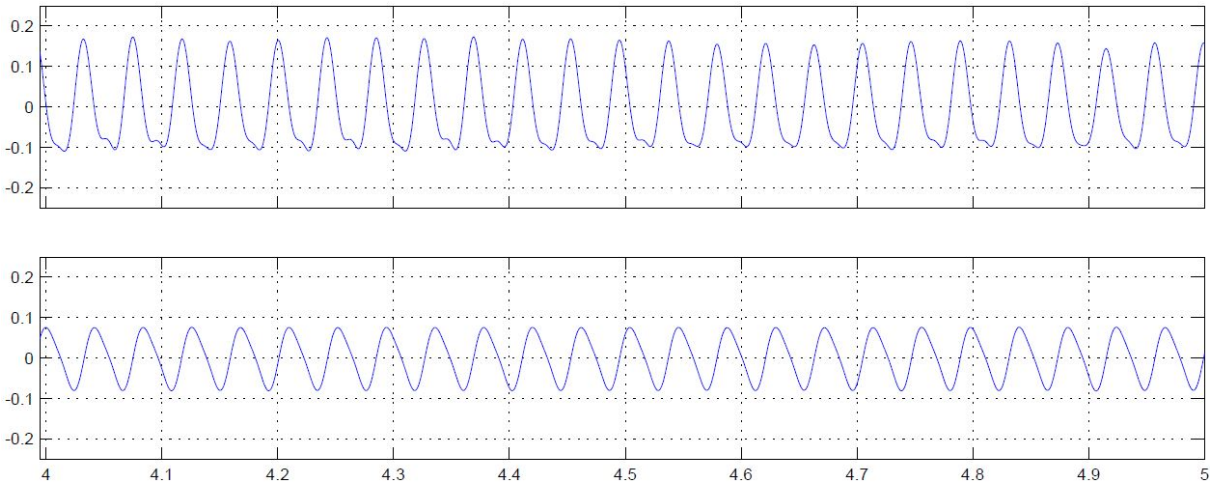

Figure 5. 4 Temporal response for acceleration (m/s^2)- t(s) in axes: a) X; b) Y

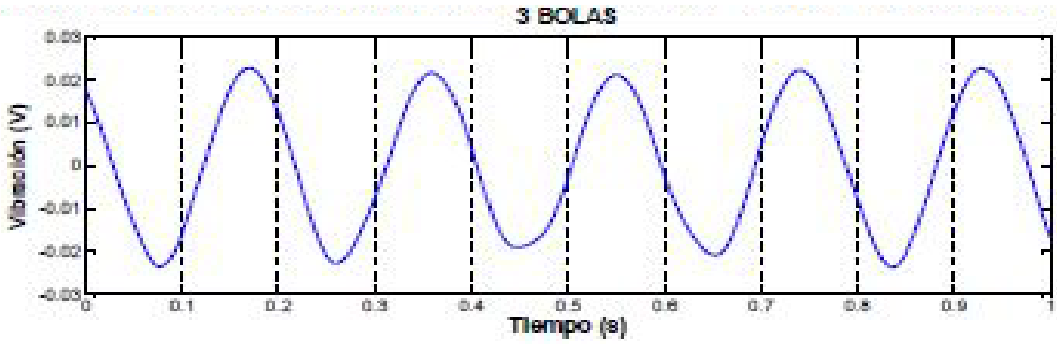

Figure 5. 5 Temporal signal of the vibration of the ball bearing wiithout faults, Load = 1500 N, rotational speed fs = 20 Hz and ms=5 kg.

Here, it is interesting to make a comparison with the model presented in [1], due to a lack of explanation of the main frequency that appears in the temporal signal of the

figure 5.5. Both models are presented under the same conditions, and the main frequency is quite different though.

The explanation for the graphic of this project is that the frequency that appears is three times the frequency of the cage, because there are three balls that roll once per revolution of the cage. The frequency of the cage, in this case, is fc=7.9348 Hz, so, the frequency of the main vibration will be 23.804 Hz, as it is shown if figure 5.4.

$$fc = \left(1 - \frac{D_{ball}}{D_{cage}}\right) \cdot \frac{fs}{2} \qquad 5.1$$

The other interesting graphic that is presented in this project, and that becomes very useful for the analysis of vibration signals, is the frequency analysis after the Fast Fourier Transform. After applying this FFT to the previous temporal situation of the 20 Hz and 1500 N, the results are shown in these graphics:

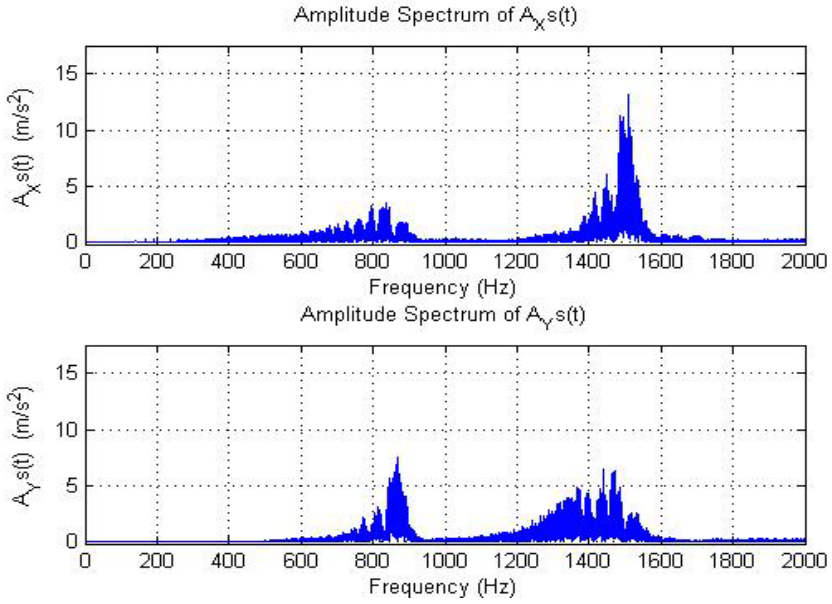

Figure 5. 6 FTT of the ball bearing with Load = 1500 N. and rotational speed fs = 20 Hz and ms = 5 kg

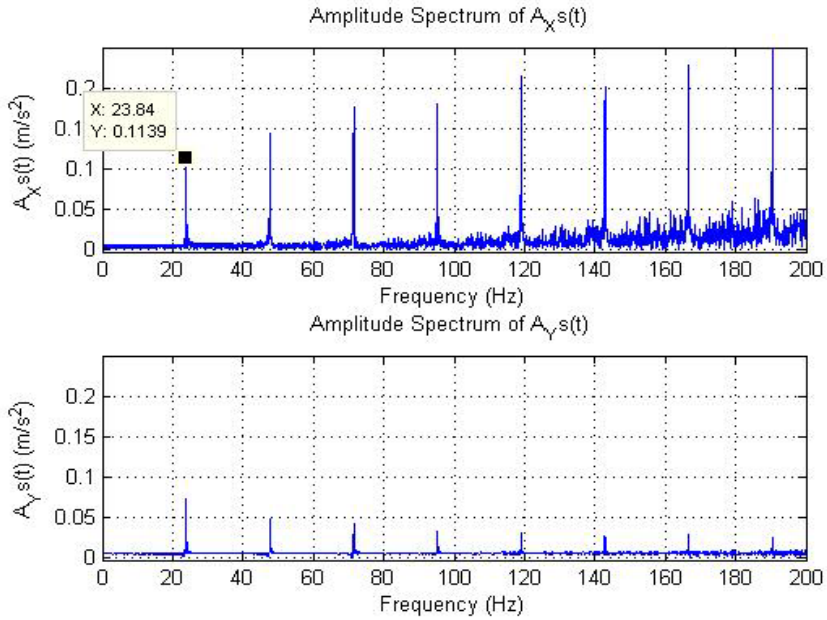

Figure 5. 7 FTT of the ball bearing with Load = 1500 N. and rotational speed fs = 20 Hz and ms = 5 kg

These both graphics above are the same. They show different ranges of frequencies.

Model of 2 d.o.f with 9 balls

For make a general comparison of both models, in figure 5.8 is presented the transitional part of the signal modelled. It is not usual have two different transitional times within the same model, and here the acceleration reaches the steady state in seven seconds while the forces seem to reach it in two.

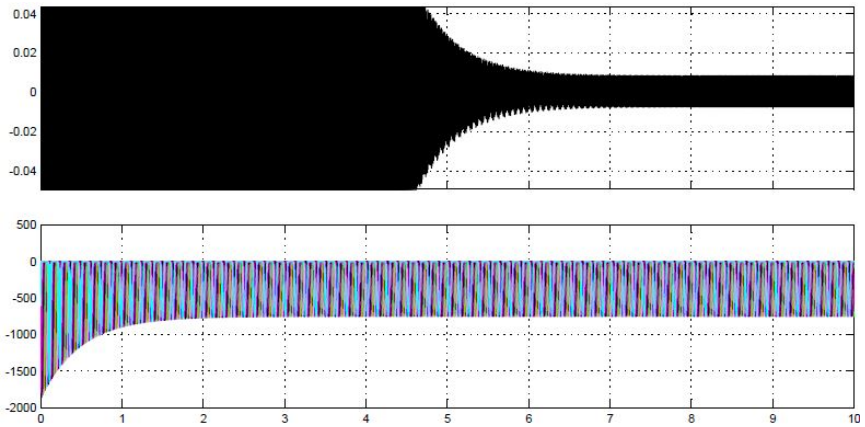

Figure 5. 8 Transitional period of time in the 3 balls model.
Graphic in Y axis of Acceleration (m/s^2) and Forces (N) – time (s)

For this model, more results are presented so a detailed explanation of its performance can be done.

First of all, as the number of the balls is too high to have clear graphics, only four balls are represented each time. Also, in order to make comparisons between different situations, a main model will be shown, figure 5.9, and then some changes will be done for the others situations. Only Y_axis will be compared in order to avoid having a too long rapport.

As it was said in the 3 balls model, the acceleration in the 9 balls model has components of higher frequency that are very relevant. However, in this one their importance is much less in steady state, as it is shown in figure 5.9 d) and e).

From the temporal response, it is also shown the FFT, where the acceleration signal can be analysed. Figure 5.10 and 5.11 show this frequency analysis where only steady state has been taken, avoiding the error introduced by transitional time. Within this figures, the main frequency can be read, and match which the frequency of 71.413 Hz obtained through the equation 4.1. This is the frequency at which all rolling elements are doing their forces as a result of passing by the 180 to 360º, that is to say the lower part of the ball bearing where the balls have to make force.

9 balls model with load of ms=5kg, Fex_y=1500N, Fex_x=0; Fu=0 and a frequency fs=20 Hz.

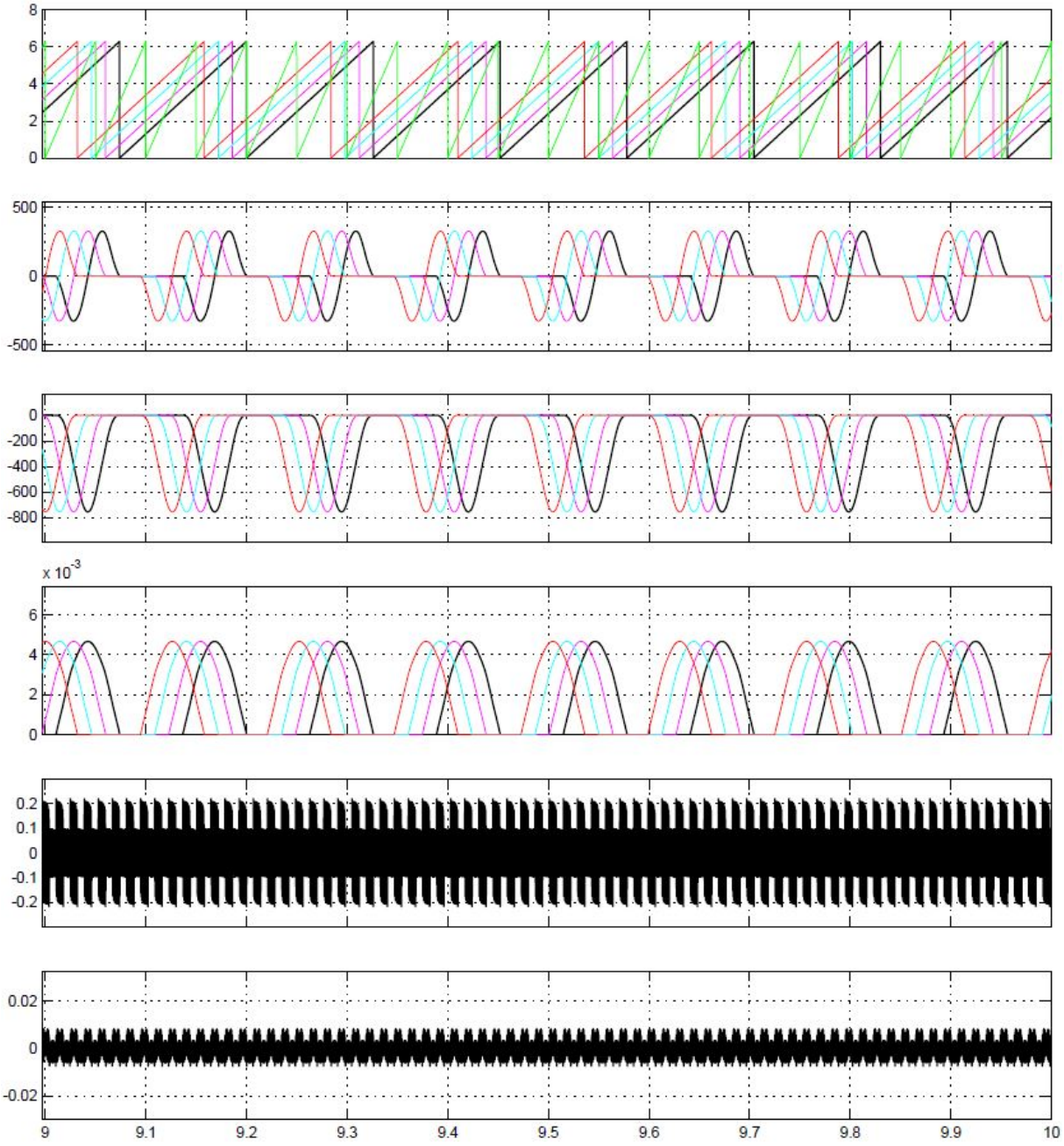

Figure 5. 9 Temporal response of: a) angles (rad), b) Forces_X(N), c) Forces_Y(N), d) delta (mm); e) Aceleration_X (m/s^2); f) Aceleration_Y (m/s^2)

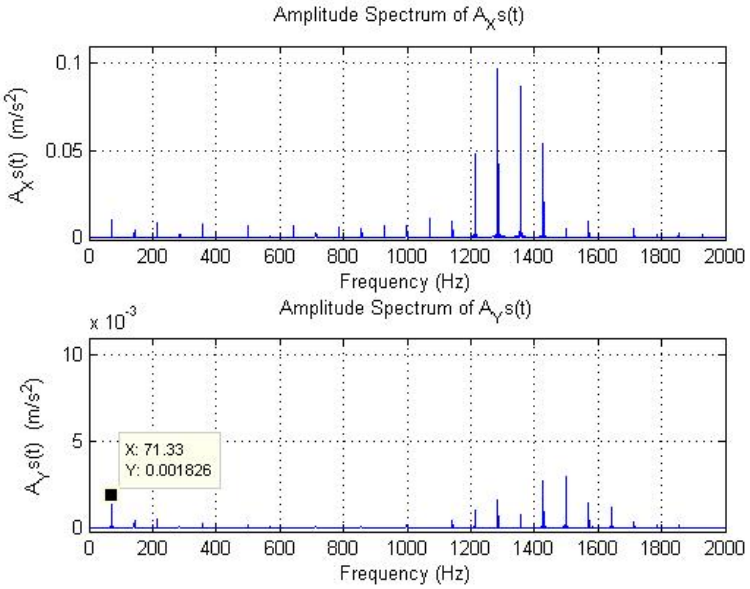

Figure 5. 10 FFT of 9 balls model

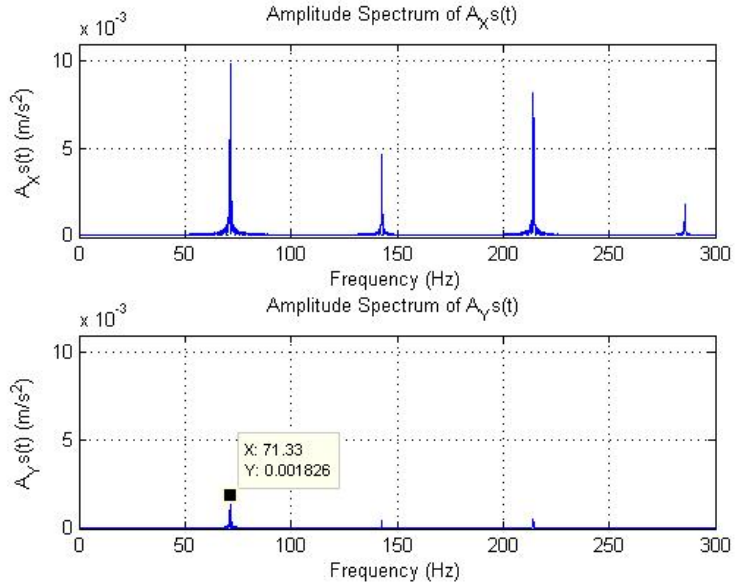

Figure 5. 11 FFT of 9 balls model zoom

As can be seen in figure 5.10, there are important high frequency components that can also be seen in acceleration signals of figure 5.9. From now, only the low frequencies graphics will be shown in the FFT analysis. There, the main frequency and their principal harmonics can be seen well. More examples of this model are shown below:

9 balls model with load of ms=5kg, Fex_y=1500N, Fex_x=0; Fu=0 and a frequency fs=28 Hz.

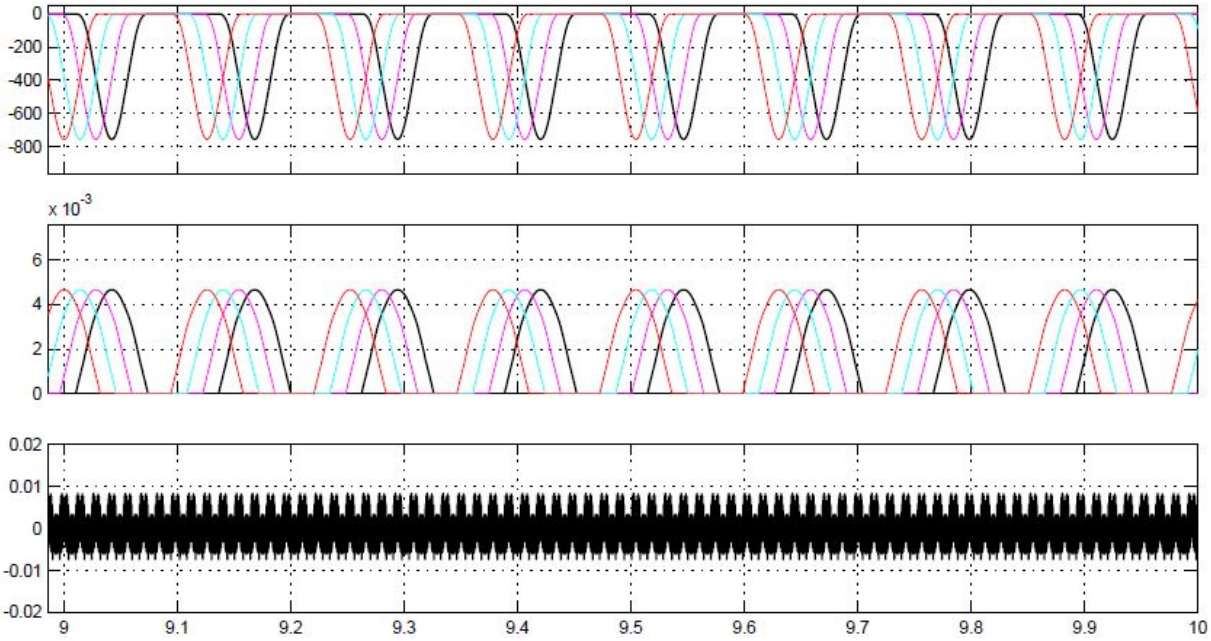

Figure 5. 12 Temporal response of 9 ball 28 hz -1500Ny: a) Forces_Y(N), b) delta (mm); c) Aceleration_Y (m/s^2)

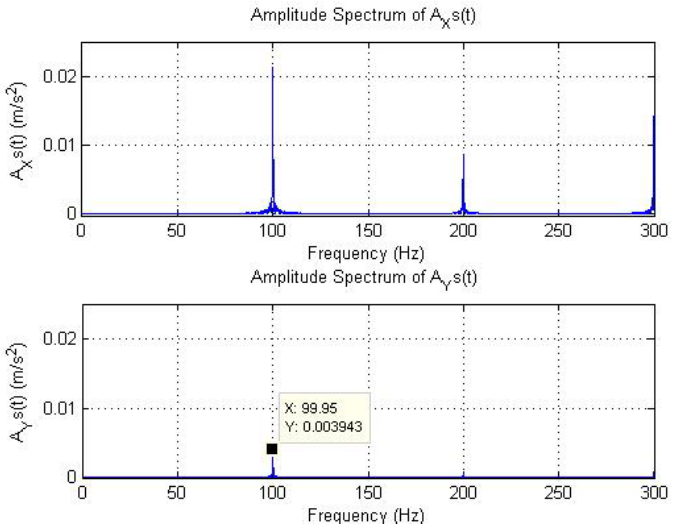

Figure 5. 13 FFT of 9 balls model, 28 Hz

The effect of increase the speed of the shaft until 28 Hz can be seen in the Figure 5.12, where both accelerations have nearly doubled the amplitude of the main frequency. Also, it is possible to verify that the amplitude of the forces have not changed, only its frequency. The main that we look for is 99.978 Hz.

9 balls model with load of ms=5kg, Fex_y=1500N, Fex_x=1000; Fu=0 and a frequency fs=20 Hz.

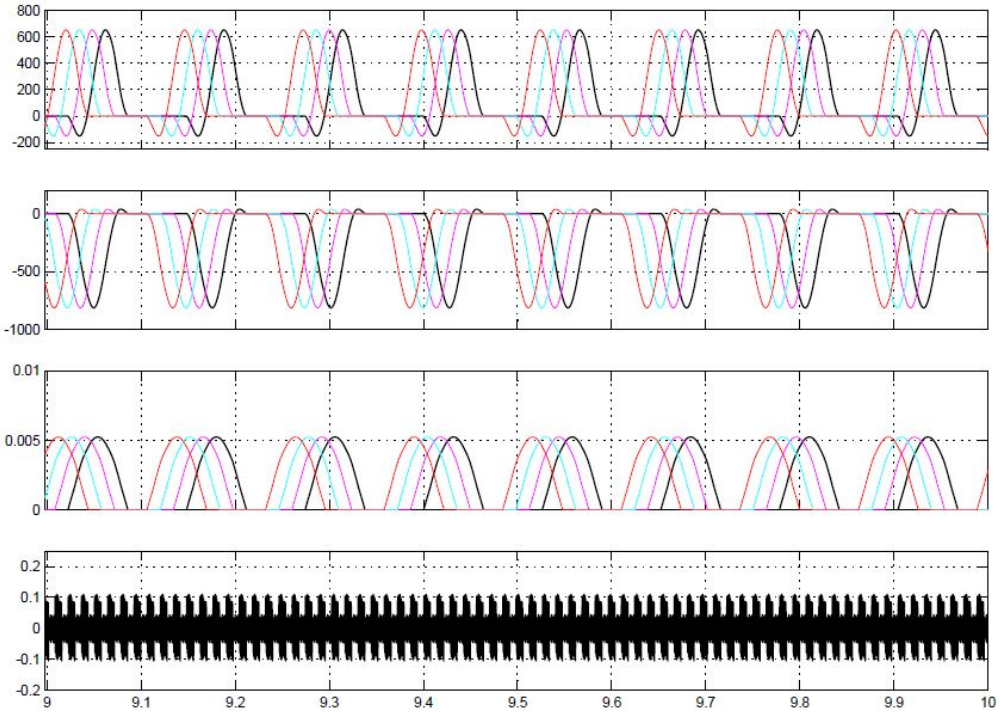

Figure 5. 14 Temporal response of 9 ball 20 Hz -1500Ny and 1000Nx: a) Forces_X(N), b) Forces_Y(N), c) delta (mm); d) Aceleration_Y (m/s^2)

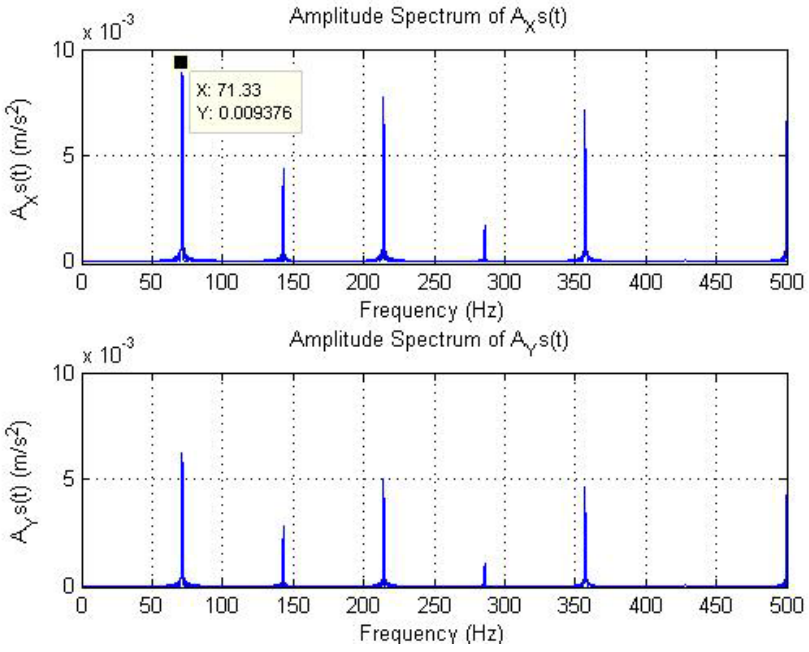

Figure 5. 15 FFT of 9 balls model, 20 Hz 1000Nx

Comparing this result with the figure 5.9, we can see the reaction of the force in X axis. This force can be applied in both senses changing the minus sign of the force.

In order to validate the model, it is necessary to see the values of the ball bearing in a certain moment. Then, they can be checked through the equation (3.9) and (3.10). An enough brief time is shown in the following figure.

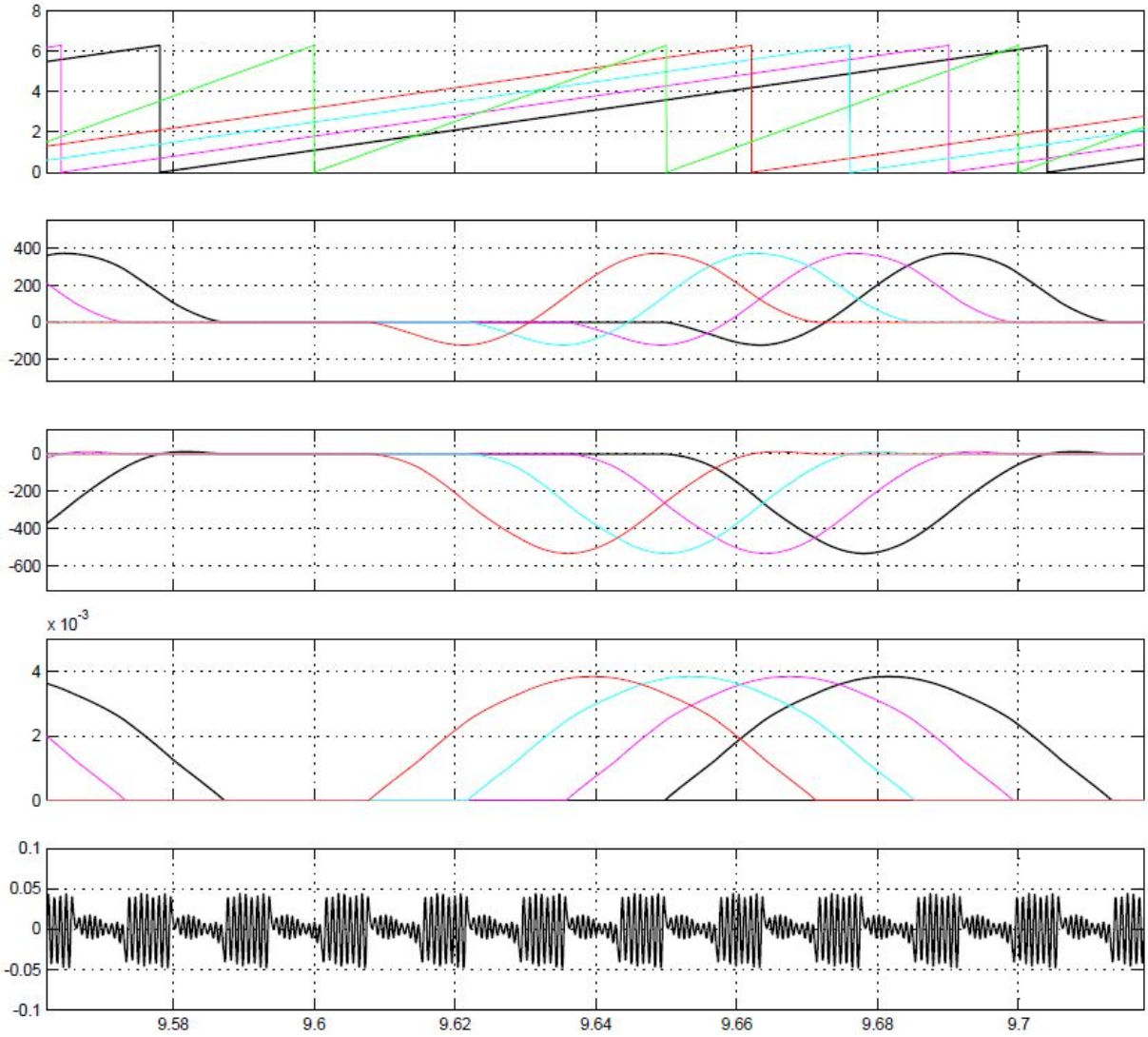

Figure 5. 16 Temporal response of 9 ball 20 Hz, punctual analysis.
a) Angles (rad), b) Forces_X(N), c) Forces_Y(N), d) delta (mm); e) Aceleration_Y (m/s^2)

At the time $t = 9.66s$:

a) $\alpha_1 = 4.082\ rad;\ \alpha_2 = 4.781\ rad;\ \alpha_3 = 5.48\ rad;\ \alpha_4 = 6.178\ rad;$
$\alpha_1 = 233.9°;\ \alpha_2 = 273.9°;\ \alpha_3 = 314°;\ \alpha_4 = 354°;$

b) $F_{x1} = -108.5\ N;\ F_{x2} = 35.1\ N;\ F_{x3} = 361.4\ N;\ F_{x4} = 212.3\ N;$

c) $F_{y1} = -149.3\ N;\ F_{y2} = -503.4\ N;\ F_{y3} = -374.2\ N;\ F_{y4} = -22.3\ N;$

f) The low frequency acceleration component at this time is $3 * 10^{-5} m/s^2$, which is approximately zero despite it is not possible to be seen in the picture above.

Finally, adding up the forces supported by the balls in Y axis, the result is $1049.2\ N$. On the other side, the forces to be supported are:

$$Fex_y = -1000\ N$$

$$m \cdot g = 5.035\ kg \cdot 9.81\ \frac{m}{s^2} = 49.39\ N$$

We can see that both sides of the equation (3.10) have the same value, so the units of the model are checked and a first validation can be made.

6. CONCLUSIONS AND FUTURE WORK

The project has focused, on the one hand, on the understanding of the current practices and methodologies of the teachers and researchers that have developed this topic before. Therefore, some books, theses and projects have been examined and accomplish to know what the current state of the technique is. Then, some models have been tried.

On the other hand, a model of ball bearing had to be chosen from the bibliography in order to implement it into Matlab and Simulink. Different models were found in other project and thesis and, after the lack of information and reliable explanations, the model developed has been a 2 d.o.f. model that allows understanding the basic dynamics of a ball bearing.

The performance of this project has allowed finding some possible mistakes in the main source of information, [1], so some changes have been proposed. These improvements will try to help into the understanding of a ball bearing as well as giving the possibility of applying these changes into more in-depth models like the 5 d.o.f. presented in the previous bibliography.

Finally, as future works, the main task would be improving the 5 d.o.f. that has given divergent results that should be fixed. It is probable that the analyses done here help into the implementations of this work.

As a continuation of the modelling of the defaults into a ball bearing, it would be interesting to implement a model like the one proposed in [13], despite is not explained well enough in that bibliography. However, this model would allow simulating the slippage as well as a gear besides the ball bearing.

The last model that could be done as the aim of an electric laboratory would be implementing within a model the effect of the vibrations over the currents and other parameters of a motor. This model would be useful because it could detect the kind of the defaults through just measuring the currents of the motor as a complement of the measuring with accelerometers.

7. REFERENCES

[1] Marín López, José María 2009, 'Análisis y Caracterización holista de un Sistema Rotativo Complejo', University Carlos III Madrid, Spain.

[2] Keith Mobley R. 2002, 'An introduction to predictive maintenance', Second Edition. Elsevier Science, USA.

[3] Ballesteros Robles, Francisco 2011 'La Estrategia predictiva en el mantenimiento industrial' Preditec /IRM

[4] Sarangi M., B. C. Majumdar, A. S. Sekhar 2004 'On the dynamics of elastohydrodynamic mixed lubricated ball bearings' Proceedings of the Institution of Mechanical Engineers, Journal of Engineering Tribology

[5] J.W. KENNEL and S.S. BUPARA. 1978, 'A simplified model of cage motion in angular contact bearings operating in the ehd lubricating regime'. Journal of Lubricating Technology.

[6] M. S. DARLOW and R. H. BADGLEY.1982, 'Early detection of defects in rolling elements Bearing'.

[7] E. D'AMATO and P. RISSONE. 1989, 'Using the envelope method to monitor rolling elements bearing'.

[8] P.D. McFadden and J.D. Smith 1983, 'Model for the vibration produced by a single point defect in a rolling element bearing', Cambridge University Engineering Department, England.

[9] H.R. HONARVAR and H.R. MARTIN. 1997 'New statistical moments for diagnostics of rolling element bearings'. Journal of Manufacturing Science and Engineering.

[10] N.and YOSHIOKA T. MORI, K.and KASASHIMA and Y. UENO 1996, 'Prediction of spalling on a ball bearing by applying the discrete wavelet transform to vibration signals'. Mechanical Engineering Laboratory, Tsukuba, Japan.

[11] C. DANTHEZ, J. M.and GIROUSSENS and R. AQUILINA 1998, 'The autocoherent spectrum: a useful spectral estimator for vibration analysis machinery. Accurate estimation and cancellation of pure tones'. ASM Ingenierie, Toulon, France.

[12] X. LOU and K. LOPARO.2004 'Bearing fault diagnosis based on wavelet transform and

fuzzy inference'. Department of Electrical and Computer Science, Cleveland, USA.

[13] N. Sawalhi, R.B Randall 2008, 'Simulating gear and bearing interactions in the presence of faults Part I. The combined gear bearing dynamic model and the simulation of localized bearing faults'.

Bai Chanquing, Xu Qingyu 2006, 'Dynamic model of ball bearings with internal clearance and waviness' Department of Engineering Mechanics, School of Aerospace, Xi'an Jiaotong University, Xi'an 710049, PR China

Dennis H. Shreve 1994, 'Introduction to vibration technology', Columbus, Ohio, USA.

Gupta Pradeep K. 1984, 'Advanced Dynamics of Rolling Elements', New York, U.S.A.

Keith Mobley, R. 2002, 'An Introduction to Predictive Maintenance', Second edition, Elsevier Science, USA.

Ming Xu, Doctor of Philosophy, 2002, 'Monitoriong rolling elements with spike energy', Ohio, USA. Site:
http://machinedesign.com/technologies/monitoring-rolling-elements-spike-energy

8. ANNEXES

Annex 1: File “Data_bearing.m”

```
ms=5.0+0.0350;  % Mass [=] Kg (motor + inner race)
g=9.81;         % Gravitational acceleration [=] m/s^2

% Stiffness constant:
    Cin=805140;        % [=] N/mm^1.5
    Cout=872780;       % [=] N/mm^1.5
    Ceq=(Cin^(2/3)+Cout^(2/3))^(3/2);
    %Ceq=Cin;

% Damping coeficient (experimental):
    D=0.01582;         % [=] Ns/mm

% Geometry % [=] mm;
    %Ball diameter
    Db=9.5;               % [=] mm;
    % Cage diameter (Ring center, ball center)
    Dc=(55.507+36.493)/2; % [=] mm;

% Rolling velocity
    % Shaft Frequency
    fs=20;             % [=] Hz
    ws=2*pi*fs;        % [=] rad/s
    % Cage Frequency
    wc=(1-Db/Dc)*ws/2; % [=] rad/s
    fc=wc/(2*pi);      % [=] Hz

% Forces
    % Disequilibrium force (radial). Cause more waviness.
    Fu=00;             % [=] N
    % External Forces on the ball bearing in X&Y axes
    Fex=-00;         % [=] N
    Fey=-200;         % [=] N

% Frequencies at which the ball passes the defect on the race
    Nb=3;       % Number of balls
    alpha=0;    % Contact angle
    % Ball Pass Freuency of the Outer race
    BPFO=Nb*fs/2*(1-Db*cos(alpha)/Dc);         % [Hz]
    % Ball Pass Freuency of the Inner race
    BPFI=Nb*fs/2*(1+Db*cos(alpha)/Dc);         % [Hz]
    % Ball Spin Frequecy
    BSF=Dc*fs/(2*Db)*(1-(Db*cos(alpha)/Dc)^2); % [Hz]
```

Annex 2: File "FFT_fromSimulink.m"

```
Inicio=length(simout.Time)/3; %Transitional period time

for Grafico=1:1
if Grafico ==1      %***Aceleración***
tx=simout.Time(Inicio:end);
Fsx=100/(tx(101)-tx(1)); % Sample frequency
ty=simout1.Time(Inicio:end);
Fsy=100/(ty(101)-ty(1));
Ax=simout.data(Inicio:end);
Ay=simout1.data(Inicio:end); a=.3;b=10*a;h=a;
end
if Grafico==2      %***Velocity***
tx=simout4.Time(Inicio:end);
Fsx=100/(tx(101)-tx(1));
ty=simout5.Time(Inicio:end);
Fsy=100/(ty(101)-ty(1));
Ax=simout4.data(Inicio:end);
Ay=simout5.data(Inicio:end); a=0.002*h;b=1.2*a;
end
if Grafico==3      %***Posición***
tx=simout2.Time(Inicio:end);
Fsx=100/(tx(101)-tx(1));
ty=simout3.Time(Inicio:end);
Fsy=100/(ty(101)-ty(1));
Ax=simout2.data(Inicio:end);
Ay=simout3.data(Inicio:end); a=0.000001*h;b=a;
end

Lx=length(Ax);
Ly=length(Ay);

NFFTx = 2^nextpow2(Lx); % Next power of 2 from length of y
Xs = fft(Ax,NFFTx)/Lx;
fx = Fsx/2*linspace(0,1,NFFTx/2+1);

NFFTy = 2^nextpow2(Lx); % Next power of 2 from length of y
Ys = fft(Ay,NFFTy)/Lx;
fy = Fsx/2*linspace(0,1,NFFTy/2+1);

% Plot single-sided amplitude spectrum.

figure(-1+2*Grafico)
subplot(2,1,1);  plot(fx,2*abs(Xs(1:NFFTx/2+1)))
    title('Amplitude Spectrum of A-V-P Xs(t) ')
    xlabel('Frequency (Hz)')
    ylabel('|A_Xs(t)|')
    axis([0,200,-a/100,a])
subplot(2,1,2);  plot(fy,2*abs(Ys(1:NFFTy/2+1)))
    title('Amplitude Spectrum of A-V-P Ys(t) ')
    xlabel('Frequency (Hz)')
    ylabel('|A_Ys(t)|')
    axis([0,200,-a/100,a])

figure(2*Grafico)
```

```
subplot(2,1,1);  plot(fx,2*abs(Xs(1:NFFTx/2+1)))
    title('Amplitude Spectrum of A-V-P Xs(t) ')
    xlabel('Frequency (Hz)')
    ylabel('|A_Xs(t)|')
    axis([0,2000,-b/100,b])
subplot(2,1,2);  plot(fy,2*abs(Ys(1:NFFTy/2+1)))
    title('Amplitude Spectrum of A-V-P Ys(t) ')
    xlabel('Frequency (Hz)')
    ylabel('|A_Ys(t)|')
    axis([0,2000,-b/100,b])
end
```